DYNAMIC OPTIMAL FRAGMENTATION WITH RATE

ADAPTATION IN WIRELESS MOBILE NETWORKS

A Dissertation
Presented to
The Academic Faculty

by

Yusun Chang

In Partial Fulfillment
of the Requirements for the Degree
Ph.D. in the
School of Electrical and Computer Engineering

Georgia Institute of Technology
December 2007

DYNAMIC OPTIMAL FRAGMENTATION WITH RATE ADAPTATION IN WIRELESS MOBILE NETWORKS

Approved by:

Dr. John A. Copeland, Advisor
School of ECE
Georgia Institute of Technology

Dr. Ye Li
School of ECE
Georgia Institute of Technology

Dr. Henry L. Owen
School of ECE
Georgia Institute of Technology

Dr. George F. Riley
School of ECE
Georgia Institute of Technology

Dr. Mostafa H. Ammar
College of Computing
Georgia Institute of Technology

To my father in heaven

ACKNOWLEDGEMENTS

TABLE OF CONTENTS

LIST OF TABLES

LIST OF FIGURES

LIST OF SYMBOLS AND ABBREVIATIONS

ARF	Auto Rate Fallback
AWGN	Additive White Gaussian Noise
BER	Bit Error Rate
CSMA/CA	Carrier Sense Multiple Access/ Collision Avoidance
CTS	Clear To Send
DCF	Distributed Coordination Function
DFE	Decision Feedback Equalizer
DIFS	DCF Inter-Frame Space
DORA	Dynamic Optimal Fragmentation with Rate Adaptation
DSSS	Direct Sequence Spread Spectrum
FCS	Frame Check Sequence
FEC	Forward Error Correction
IFS	Inter-Frame Space
ISI	Inter Symbol Interference
ISM Band	Industrial Scientific and Medical Band
MAC	Medium Access Control
MPDU	MAC Protocol Data Unit
MSDU	MAC Service Data Unit
OAR	Opportunistic Auto Rate
OFDM	Orthogonal Frequency Division Multiplexing
PCF	Point Coordination Function
PER	Packet Error Rate
RBAR	Receiver-Based Auto Rate

RTS	Request To Send
RTT	Round Trip Time
SIFS	Short Inter-Frame Space
TCP	Transmission Control Protocol
UDP	User Datagram Protocol
WLAN	Wireless Local Area Network

SUMMARY

Dynamic optimal fragmentation with rate adaptation (DORA) is an algorithm to achieve maximum goodput in wireless mobile networks. With the analytical model that incorporates number of users, contentions, packet lengths, and bit error rates in the network, DORA computes a fragmentation threshold and transmits optimal sized packets with maximum rates. To estimate the SNR in the model, an adaptive on-demand UDP estimator is designed to reduce overheads. Test-beds to execute experiments for channel estimation, WLANs, Ad Hoc networks, and Vehicle-to-Vehicle networks are developed to evaluate the performance of DORA.

DORA is an energy-efficient generic CSMA/CA MAC protocol for wireless mobile computing applications, and enhances system goodput in WLANs, Ad Hoc networks, and Vehicle-to-Vehicle networks without modification of the protocols.

CHAPTER 1

INTRODUCTION

The demand for broadband wireless communication has been increasing, and ubiquitous wireless access to Internet is a challenging problem. To accommodate these requests, wireless systems should work well in typical wireless environments, characterized by the path loss of the signals, multi path fading, interference to adjacent channels, and random errors.

CSMA/CA MAC is a carrier-sense multiple access protocol with collision avoidance to share the medium, and wireless local area networks (WLAN) that use the protocol have provided high data rates, far exceeding that offered by the third generation (3G) networks. However, the CSMA/CA MAC is not efficient in the unlicensed ISM band, which is vulnerable to noise generated by TVs, microwaves, and cordless phones.

In this research, dynamic optimal fragmentation with rate adaptation (DORA) is developed to enhance system goodput in time varying wireless mobile networks. The number of contending stations, packet collisions, packet error probabilities, and fragmentation overheads are modeled in the analysis. Using an adaptive SNR estimator, the sender estimates the SNR of the receiver, and shapes arbitrary sized packets into optimal length packets with maximum transmission rates. The performance of DORA is evaluated by implemented test-beds, which consist of CISCO access point (Aironet 1231-G-A-K9) with mobile stations in WLAN, four mobile stations in multi-hop ad hoc networks, and vehicle-to-vehicle networks.

1.1 Origin and History of the Problem

The desire for ubiquitous wireless connectivity is growing rapidly these days. Third generation (3G) network industries are accelerating the development and

deployment of wireless data networks. Built on cellular technologies, it promises wide coverage, seamless support of mobility, paging, and quality of service. However, it is a complex and costly connection-oriented networking that provides approximately 2 Mbps for indoor traffic.

To meet demands of high data rate users, many companies have provided wireless local area networks (WLAN) that theoretically give up to 54 Mbps. Since it uses the unlicensed spectrum with a simple design, the cost is much lower than 3G networks. On the other hand, WLAN covers less than a few hundred meters and mobile users are unable to have a seamless connection when moving to other networks. Users in the future are expected to use both types of networks, one for wide coverage and reliable seamless connection, and the other for high data rate with low cost.

The low costs of wireless cards and access points of WLAN made it possible to use at home, in university access networks, and at hotspots such as train stations, hotels, coffee shops, and airports. One of the most common and prevalent wireless LANs is the IEEE 802.11b [1] network that can achieve 11 Mbps. However, the actual data rate may vary and depends on network configurations, channel states, and user behavior. Intersymbol interference (ISI) caused by multipath fading is known to be the major obstacle to high-speed data transmission. To counter the ISI, the receiver adopts the decision feedback equalizer (DFE) to compensate deep spectral nulls in frequency selective time dispersive channels. However, many vendors claim less than a 100-ns delay spread for full–speed 11 Mbps performance at a reasonable frame error rate. When the delay spread is large, many cards reduce the transmission rate, and results in degradation of the throughput. In addition, it shares 2.4 GHz ISM band with other electronic devices, such as TVs, microwaves, cordless phones, and Bluetooth devices. Since the spectrum is inherently wide open to the interference from these devices, and no

forward error correction (FEC) is used, it is not surprising that actual network throughput is far less than 11 Mbps. To support higher rate date transmission in wireless LAN, the IEEE 802.11a [2] is proposed to provide data rate up to 54 Mbps using orthogonal frequency division multiplexing (OFDM) in 5 GHz. Even though, the spectrum is not much crowded as in 802.11b, the line of sight propagation characteristics prohibit achieving the theoretical maximum throughput. Typically less than 20 Mbps can be obtained in normal traffic conditions in 25 meters. To avoid a large propagation loss and the line of sight characteristics, the IEEE 802.11g [3] standard has been finalized to support 802.11a/b physical layer modules in 2.4 GHz. However, it uses the same congested spectrum, and the data rate drops down to the 802.11b in the presence of an 802.11b participant in the network.

1.2 Related Work

Rate adaptation schemes have been proposed to increase the throughput of WLAN by changing the transmission rate to the time varying wireless channels while satisfying a given bit error rate (BER) or packet error rate (PER). The auto rate fallback (ARF) protocol [4], which selects the transmission rate of the sender based on how many consecutive successful transmissions have been received, was adopted in the commercial product, Lucent WaveLAN II. Simply counting the number of successful and unsuccessful transmissions to decide next transmission rates has inherent limitation to better suit time varying nature of the channels. The receiver-based auto rate (RBAR) [5] proposed using the RTS/CTS handshaking for exchanging link quality. The receiver estimates the channels from the received signal strength of the RTS frame, and feedback this information in the modified CTS header to the sender for selecting the next transmission rate. From accurate estimation of the channel, the RBAR yields significant

performance benefit compared to the ARF. However, this approach requires RTS/CTS exchange, and sacrifices bandwidth when there are no hidden terminals in the network. In addition, protocol modification makes it difficult to be deployed in reality. The opportunistic auto rate (OAR) [6] extends the RBAR such that it ensures the same time-shares for the all nodes. In a good channel, it opportunistically sends more packets while maintaining the same channel access time. Nevertheless, it has inherent problems of protocol modification and bandwidth waste as in RBAR.

Packet length adaptation is another approach that has been studied to increase the throughput of WLAN by changing the frame size to the time varying wireless channels. If transmitters break messages into smaller fragments for sequential transmission, the shorter duration of each fragment has a better chance of escaping burst interference and increases throughput. This simple technique also reduces the need for retransmission in many cases and can be used to reshape arbitrary sized packets into optimal length packets to improve wireless network performance. The 802.11 standard mandates all receivers support fragmentation, but it leaves such functionality optional on transmitters. Full-time fragmentation in a transmitter makes it possible to design a less expensive receiver resulting in lower receiver sensitivity. However, it incurs overhead on every fragment rather than every frame, thereby reducing the aggregate throughout of the WLAN and the realizable peak throughput rate achieved between stations.

The architecture for adapting the frame length to the time varying channel is proposed in [7]. It exploits the effect of BER and frame length on throughput in wireless network. Simple backoff based frame length adaptation [8] is proposed to adapt fragment sizes using the fragmentation threshold in time varying error prone channels. In this

algorithm, the next fragmentation threshold is set to half of the previous one, if ACK is lost or time out. When the transmission is successful, it is doubled in the next stage. Similar approaches, [9] and [10], are proposed to tune fragment size to fit in a dwell time in the frequency hopping system. However, these all approaches are for a general MAC protocol, and it does not include 802.11 distributed coordination function (DCF) protocol to calculate optimal fragmentation. In [11] and [12], a link adaptation strategy is studied to select the optimal combinations of the 802.11a [2] PHY mode and the fragment size to achieve the best goodput performance for different SNR conditions. This approach has a detailed analysis of DCF with fragmentation, and shows how the fragmentation affects goodput with different physical modes and SNR. Although the scheme achieves some degree of optimization, it excludes the effect of collision, which has the same impact on the exponential backoff procedure of the DCF. When we consider collisions in the network, random packet drops are not solely due to a bad channel, and thus not the only reason of an ACK lost or time out. Therefore, contention based packet-sending probability and collision probability requires to be incorporated in the calculation of the goodput. J. Yin et al models the effect of the contentions among users, the collisions, and the random errors at the receiver in [13]. The analysis computes the optimum packet size to maximize the throughput in an error prone channel. However, the MAC layer is not capable of reshaping arbitrary sized packets to the optimum sized packets, and if we apply fragmentation, the optimal fragment size will be different because of the fragmentation overhead and time spent for the transmission.

Rate adaptive protocol with dynamic fragmentation [14] combines fragmentation with existing rate adaptation schemes. Basic operation of the protocol is similar to RBAR

[5] in that it exchanges channel information using modified RTS/CTS packets. In fragmentation, the time duration for transmitting each fragment is equal to each other by adjusting the length of each fragment to available rates. For example, if a channel becomes better during the fragmentation process such that the next transmission rate is doubled, the next fragment length is also doubled to send twice as much data, while the time spent to transmit those two fragments remains the same.

Although, this algorithm achieves much better throughput compared to RBAR [5], it has the same problems of rate adaptation approaches. In addition, the typical WLAN channel is slow fading, and the channel coherent time is long enough to hold multiple packet transmissions. Therefore, actual performance benefit of this algorithm in a typical indoor WLAN is limited, while incurring control packet overheads and protocol change in existing deployed 802.11 systems.

CHAPTER 2

SYSTEM ANALYSIS

2.1 CSMA/CA MAC Analysis

The fundamental access method in the IEEE 802.11 medium is DCF, a carrier sensing multiple access/collision avoidance (CSMA/CA) mechanism to avoid collisions in the medium while users contend to access the channel. If contention free access is required, point coordination function (PCF) built on the top of the DCF can be provided.

In DCF, stations sense whether the medium is idle or occupied by other stations
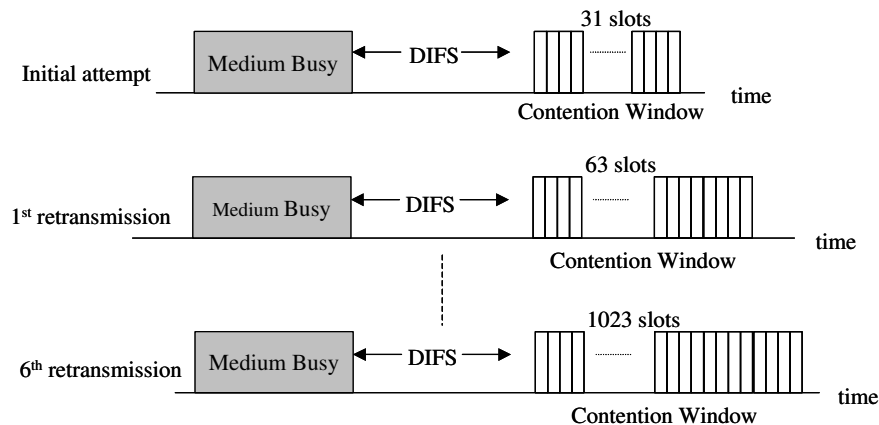
Figure 1. Exponential backoff of the contention window.

before sending data. If the medium is idle for a DCF inter-frame space (DIFS) interval, the station decreases its backoff timer, which is randomly selected at the first attempt of the transmission. When the backoff timer expires, it transmits data. If the transmission is successful, the station resets the backoff timer and chooses a new time slot in the contention window. A station that has failed the first round of transmission should

7

exponentially backoff the contention window and retry later when the medium is idle. This exponential backoff of the contention window will repeat until it reaches its maximum of 1023 slots for the 802.11b direct sequence spread spectrum (DSSS) physical layer as in Figure 1. Then it remains there unless the timer is reset by a successful transmission, or discarded by the retry counter. Because DCF operates without a central coordinator, the medium access control is done independently. This typical exponential backoff ensures the stability of the network and guarantees long-term fairness even in the maximum saturated traffic with many contending stations in the same BSS.

Figure 2 depicts how the DCF works with different inter-frame spaces defined in the IEEE 802.11 standard. If the medium idles longer than the DIFS interval, stations sensing the medium attempt to get access when their backoff timers expire. If only one
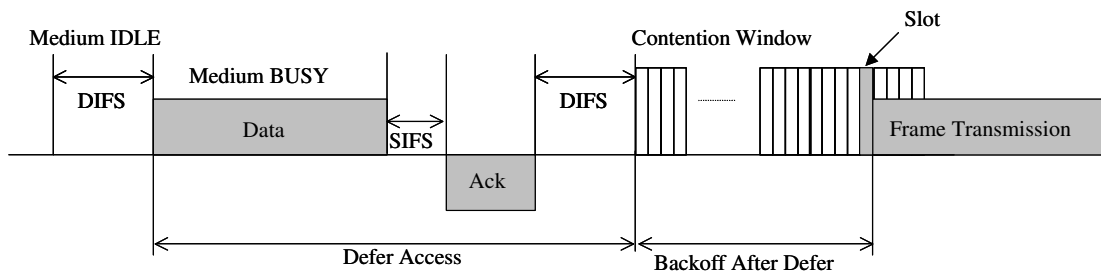
Figure 2. Basic access method and inter frame space.

station tries to access the channel when no other stations transmit data or interfere the sender, the station captures the channel for transmission. After successfully transmitting, the acknowledgement is returned within the SIFS (Short IFS) from the receiver. The contending stations freeze the backoff counter and defer the transmission during this period. If the medium is released and idle for the DIFS interval, other contending stations

start counting down the backoff timers and follow the procedure described above to access the channel.

Consider DCF under saturated traffic conditions to analyze the performance of 802.11 CSMA/CA MAC. In [15], a complicated Markov model is presented to employ exponential backoff in the assumption of ideal channel conditions. However, the 802.11 ISM band is inherently vulnerable to interference from other electronic devices. To implement DORA with low computational complexity, a comprehensive analytical model that considers fragmentation overheads and time intervals is proposed to generalize the model suggested in [13]. Even though the methodology to derive the formula is similar to [13], the actual computation of the optimal packet length is different due to fragmentation overheads and time components. Furthermore, packet lengths and transmission rates are changing dynamically in DORA while [13] is a simple calculation of the packet lengths in static environment.

Each time a station transmits a packet, assume that the unsuccessful transmission probability p is constant at steady state in a generic slot. The key assumption is that p, which is the resultant from collisions or corrupted random bits, is a constant and independent probability seen by a packet being transmitted in a randomly chosen time slot. This is a valid assumption if backoff stage of the whole system with nodes n and random bit errors is at steady state. Define W_i is the contention window after i times of collision. Then, W_i is

$$W_i = (W_m * 2^i) - 1,$$
(1)

where W_m is 32 in the initial round of transmission as in Figure 1. The backoff timer chooses a time slot uniformly between 0 to W_i after i times of collision until the packet is successfully transmitted or discarded by the retry counter. In the same BSS, the probability of unsuccessful transmission can be denoted as p in n contending nodes. Then, the probability of success for each station after i times failure is

$$P_{success}(i) = (1-p)\, p^i \; . \tag{2}$$

The calculation of the average waiting time $\overline{W}$ for a station to transmit a packet can be expressed with the equation (2) and the average contention window size $\frac{W_i}{2}$. That is

$$\overline{W} = \sum_{i=0}^{RC} (\frac{W_i}{2})\, P_{success}(i) \; , \tag{3}$$

where RC is the retry counters defined in [1].

Assume the average packet transmission probability of each node P_τ, which covers the whole backoff stage, can be calculated as a constant value at steady state, the average probability of each station to send a packet, P_τ [17] can be represented as

$$P_\tau = \frac{1}{(\overline{W}+1)} \; . \tag{4}$$

Consider the collision probability of a station to transmit a packet while competing with other $n-1$ stations. The collision probability p_c can be expressed as

$$p_c = 1-(1-P_\tau)^{n-1} . \tag{5}$$

The integrity of the 802.11 frames is checked at the receivers by the frame check sequence (FCS). The receivers calculate the FCS to include the MAC header and frame

body, and compare it to the received FCS. If a frame passes the integrity check, there is a high possibility that the frame was not damaged in transit. If it fails, the packet was corrupted by collisions, or random errors due to interference and poor SNR. Therefore, the probability of unsuccessful transmission should include both the collision probability, p_c, and packet loss due to random bit error. This random bit error probability is denoted as p_b for BER in wireless channels. Then, the upper bound of the probability of the packet loss [18] by random bit errors in an L bit packet can be expressed as

$$p_e = 1 - (1 - p_b)^L. \tag{6}$$

Assume p_c and p_e are independent, the probability of unsuccessful transmission p is given as

$$p = 1 - (1 - p_e)(1 - p_c) \tag{7}$$

Using (1) to (7) with a given number of users n, BER, and L-bit long packets, the two unknown values, p and p_c can be solved using numerical techniques. Assuming the probability of a successful transmission when there is at least one station to transmit, the probability that there is a transmission among n stations in the channel is $1 - (1 - P_\tau)^n$. Since only one station transmits while other $n - 1$ stations keep quiet, the probability of successful transmission without collision is given by [13].

$$P_s = \frac{n P_\tau (1 - P_\tau)^{n-1}}{1 - (1 - P_\tau)^n}. \tag{8}$$

11

2.2 Fragmentation Analysis

Fragmentation is a simple technique to enhance the performance in a wireless
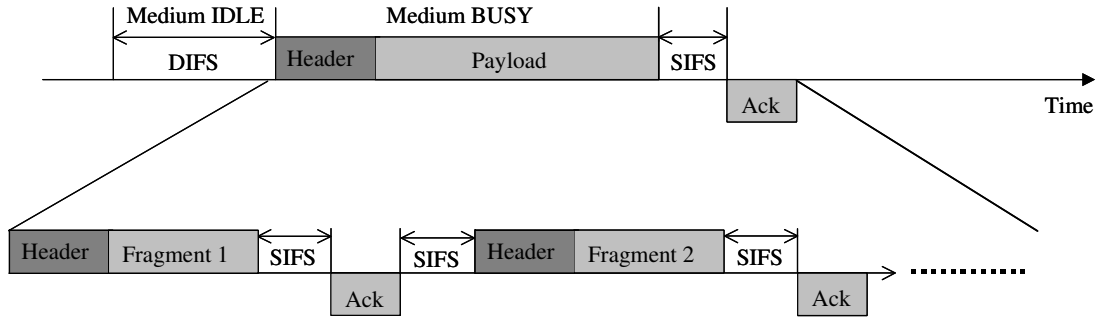
Figure 3. Fragmentation operation.

channel. Consider the impact of important network parameters, such as packet length,

number of users, contentions, collisions, and random errors on the goodput performance.
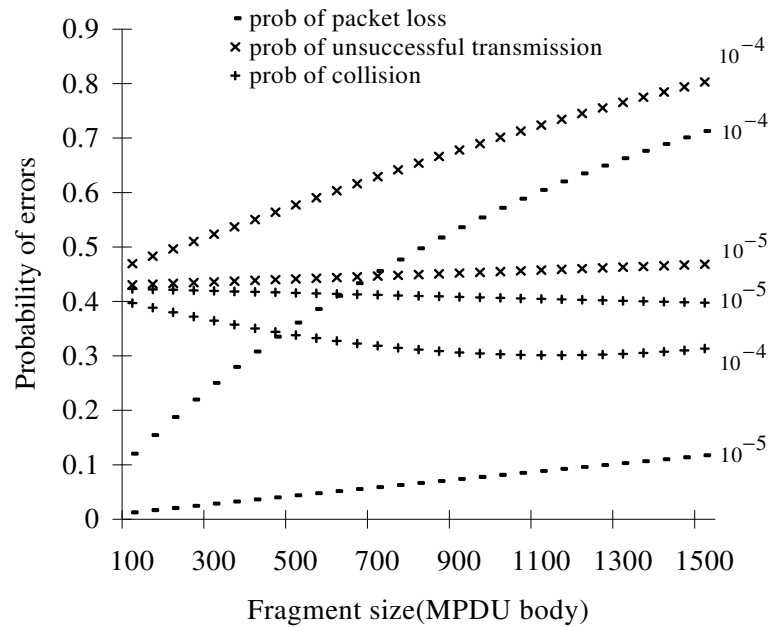
Figure 4. Probability of errors and BER.

Fragmentation incurs an overhead as seen in Figure 3. If an L bit long packet with packet header, H, is fragmented j times L_{opt}, it incurs $j-1$ times of additional overhead of $H + 2SIFS + ACK$. As the number of fragmentation grows, the number of overhead also additively increases, while p_e is exponentially reduced from $1-(1-p_b)^L$ to $1-(1-p_b)^{L_{opt}}$. This packet loss due to wireless random errors has a big impact on unsuccessful transmission probability, p, especially when the channel becomes worse. As illustrated in Figure 4, p_e is dominant when the BER is 10^{-4}, whereas p_c has the dominating effect on p at a moderate BER of 10^{-5}. For the same fragment with a given n, stations have a smaller p_c at 10^{-4} than that of 10^{-5}. In other words, collision probability in a bad channel is lower than a good channel. The rational is that an unsuccessful probability, p, is greater in a bad channel, (e.g. 10^{-4}) than a good channel (10^{-5}), and p_e is higher at 10^{-4} due to the dominant influence of the random errors. Thus, it causes a larger average waiting time $\overline{W}$ in a bad channel, and consequently the collision probability decreases due to the exponential backoff algorithm. However, the effects of the fragment size on p_c decrease for a higher SNR values, and p_c primarily relies on the number of users rather than BER in this channel.

In Figure 5, the fragment size has a direct impact on it for the same BER of 10^{-5}. Note that the smallest p does not guarantee a maximum goodput unless the fragment length is considered, and this is where the optimization is required for p, fragment size, BER, and the number of users n in a given transmission rate.
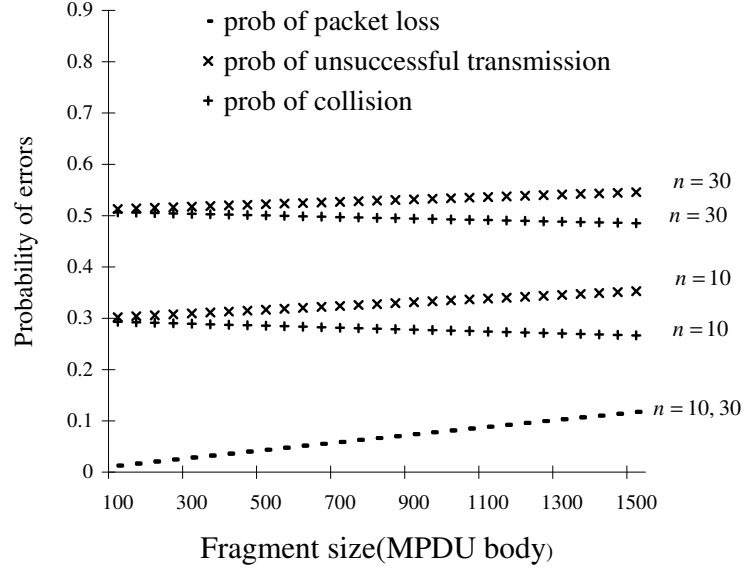
Figure 5. Probability and number of users.

2.3 Goodput Analysis

Consider goodput as the fraction of time that the medium is occupied to transmit user data successfully. Various time components to obtain goodput formula taking into consideration of fragmentation can be derived. The average idle time between two consecutive transmissions can be defined as t_{idle}. Then, t_{idle} can be represented by the mean of geometric distributions [13]

$$t_{idle} = \frac{1}{1-(1-P_\tau)^n} - 1.$$

(9)

Assume sending an L bit packet with data rate R and packet header H'. The time duration t_s is normalized to a slot time while transmitting user data. Then, t_s can be represented as

14

$$t_s = \frac{L - H'}{R * t_{slot}},$$
(10)

where H' is physical, MAC, and TCP/IP layer headers. The time interval t_f to send an

L bit packet successfully with fragmentation can be calculated with different inter-frame

spaces (IFSs) and overhead of the packet during the fragmentation procedure. Consider

the fragmented packet that maximizes goodput as L_{opt}, and physical and MAC layer

headers, H. If an L bit packet is fragmented into j packets of size L_{opt}, an additional

overhead of $(j-1)(H + 2SIFS + ACK)$ is added. Since the total amount of information in

an L bit packet after fragmentation is the same with the overhead H, the time interval

t_f can be expressed as

$$t_f = DIFS + L + SIFS + ACK + (j-1)(H + 2SIFS + ACK).$$
(11)

If there is collision in the network, the time duration to detect the collision in

fragmentation t_c, is

$$t_c = DIFS + L_{opt} + SIFS + ACK.$$
(12)

Consequently, the goodput G can be expressed in the following formula.

$$G = \frac{P_s \cdot (1 - P_e) \cdot t_s}{t_{idle} + P_s \cdot (1 - P_e) \cdot t_f + (1 - P_s) \cdot t_c + P_s \cdot P_e \cdot t_f}.$$
(13)

Given a packet size L, the number of users n, the BER, and the transmission rate, the

solution of the nonlinear system L_{opt} can be uniquely determined using numerical

approaches to find where G reaches the maximum value.

The optimal fragment length (frame body of MPDUs) for 1500 bytes MSDU is illustrated in Figure 6 with various BERs and number of users for 1Mbps modulation rate in 802.11b. In a perfect channel with less than 10 users, fragmentation has no positive impact on goodput. Since the probability of random packet loss is negligibly small in this channel, an unsuccessful transmission probability p is almost equal to the collision probability p_c in (7). In the previous section, p_c is not a function of packet length if the channel is perfect. However, it is a function of number of users in the network. Therefore,
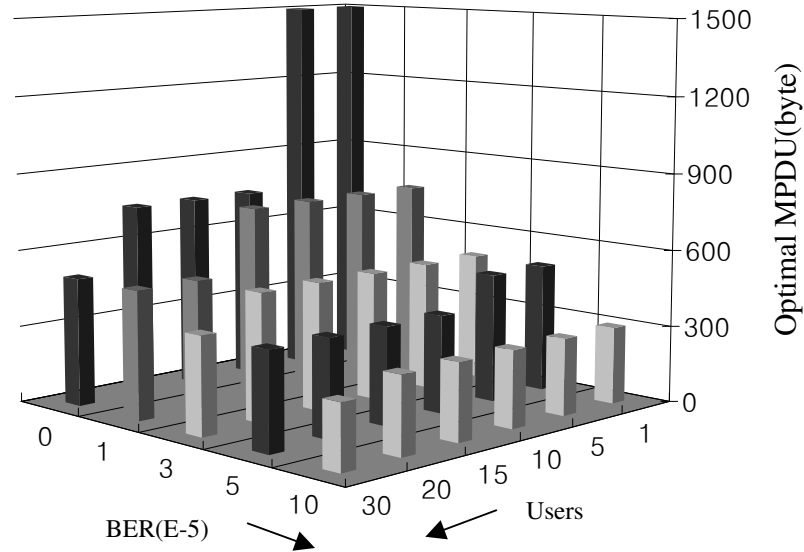
Figure 6. Optimal MPDU for 1500 bytes MSDU with BER and number of users.

if there is no hidden terminals and interference at the receivers, and all stations obey the basic access rules, a constant p_c is expected regardless of the packet length, and the performance will be degraded gracefully. However, p_c increases as the number of user increases. Thus, a longer packet needs more time to detect loss and recover from it. As

16

the contentions become severe, the optimal fragmentation provides more benefit by adjusting the fragment size to the channel. As the channel error becomes worse, the fragment size should decrease abruptly to compensate the random errors. The contention among users also affects the optimal fragment size as mentioned earlier. However, the
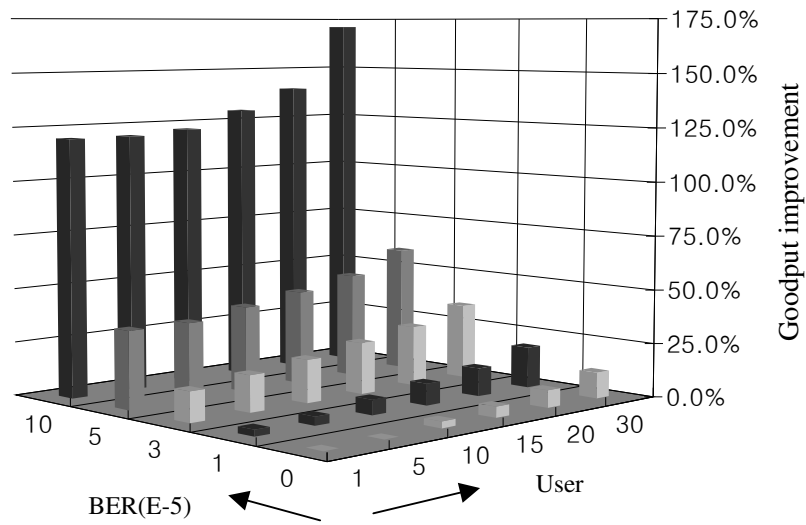
Figure 7. Goodput improvement of optimal fragmentation over non-fragmented transmissions.

impact of the contention is smaller, since random errors play bigger role on the exponential backoff procedure than the collisions caused by contentions. Consequently, optimal fragmentation improves goodput more effectively as the channel becomes worse, or the number of user increases in the network. The performance of the optimal fragmentation is illustrated in Figure 7 and Figure 8 for the 1 Mbps 802.11b physical mode.

17
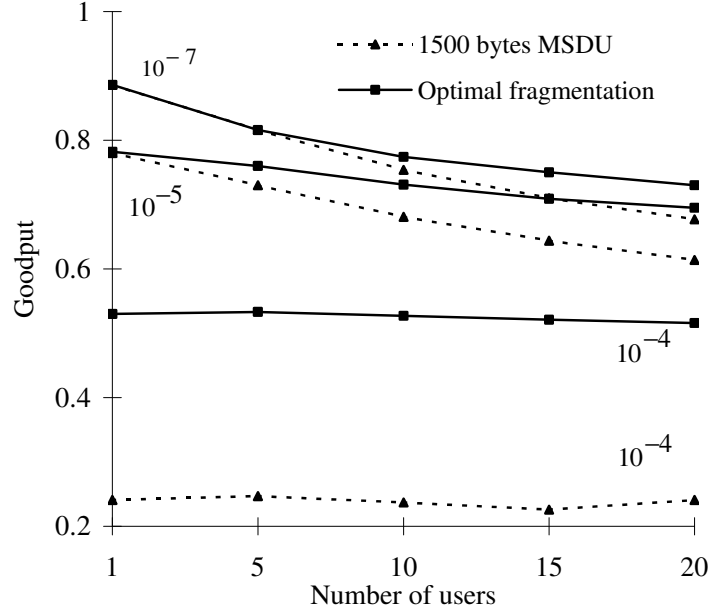
Figure 8. Goodput comparison for number of users.

2.4 Delay Analysis

Packet delay is also an indicator of the performance matrix. For each user to send a packet with n contending nodes, if we assume each node shares equally the average stationary goodput, the delay for a node to transmit a bit is n/G. Since the time to send user data in a packet is given at (10), the packet delay D_{packet} is

$$D_{packet} = \frac{n}{G} t_s . \tag{14}$$

Figure 9 shows the packet delay for the 1500 bytes MSDU in 802.11b [1], 1Mbps DBPSK physical mode. As the number of user grows, the delay performance is deteriorated proportionally. For an example of a typical WLAN environment having 20 users with BER of 10^{-5}, the network will experience 380 ms of packet delay for normal

operation, and 330 ms for the optimal fragmentation. This yields a 13.15% performance

gain. The performance gain of the optimal fragmentation increases as the channel errors

become worse. In this example, it yields 33.16% delay performance improvement for a

BER of 5×10^{-5}.
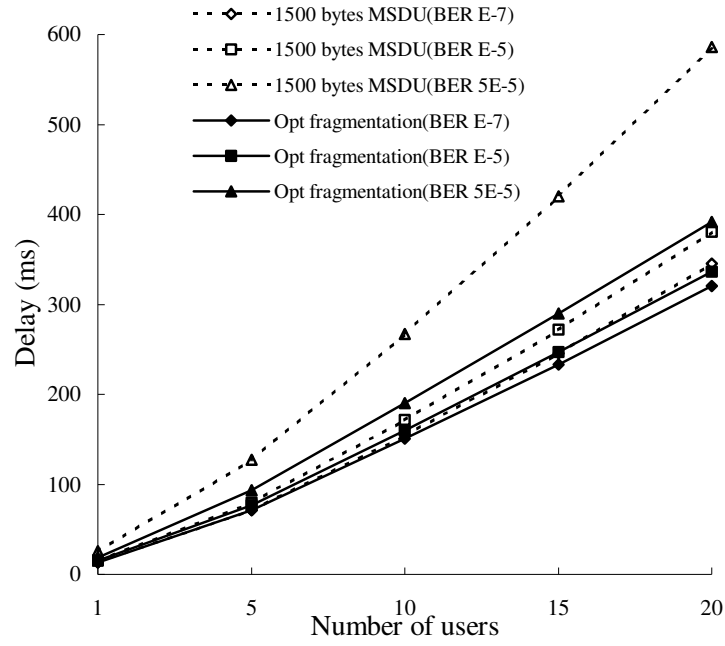
Figure 9. Packet delay for 802.11b 1Mbps, DBPSK physical mode.

CHAPTER 3

DORA DESIGN

Optimal fragmentation significantly improves goodput in a typical wireless environment. To apply optimal fragmentation dynamically in time varying channels, the sender should be informed of the SNR of the receiver. Dynamic optimal fragmentation with rate adaptation (DORA) uses the SNR estimator with network parameters to select the maximum rate and the optimal fragmentation. The network parameters considered in the model includes the incoming packet length, BER, number of users, and the transmission rates. In this chapter, design considerations to implement DORA will be discussed with rate adaptation and channel estimation algorithm.

3.1 Optimal Fragmentation

The optimal fragmentation enhances goodput and delay performance in typical wireless environments as stated earlier. The actual values to be used in the system should consider MAC header and SNAP header. Assuming the optimal fragment, L_{opt}, is 500 bytes for 1500 bytes MSDU, the fragmentation threshold should be 528 bytes taking into consideration of the 28 bytes of the MAC header. An additional 8 bytes of SNAP header are required in the last fragment. Therefore, the threshold for the MSDU is three 531 bytes MPDUs that carry 3 additional bytes for the SNAP header in each fragment.

The problem is how to monitor these parameters in real time, such as incoming packet length, BER, number of users, and transmission rates, in order to decide optimal fragmentation threshold without modifying the protocols. Packet length and number of users are known parameters in the network. For the BER and transmission rates, a new rate adaptation algorithm is proposed to incorporate optimum rate with the optimal

fragmentation to meet the desired BER or packet error rate (PER). In the following section, DORA rate adaptation will be elaborated.

3.2 Rate Adaptation

Different modulation schemes support different rates. Thus, the rate can be adjusted to improve network goodput by switching to a higher modulation scheme if channel conditions improve. Figure 10 illustrates the BER vs. SNR curves for various modulation schemes. These curves can be found for 802.11 physical modes in [19, 20, 21]. The target BER can be maintained by simply switching rates. With the consideration of the rate for a given SNR in Figure 10, the rate R may be written as

$$R = R_i, \; SNR_i \leq SNR < SNR_{i+1}. \tag{15}$$
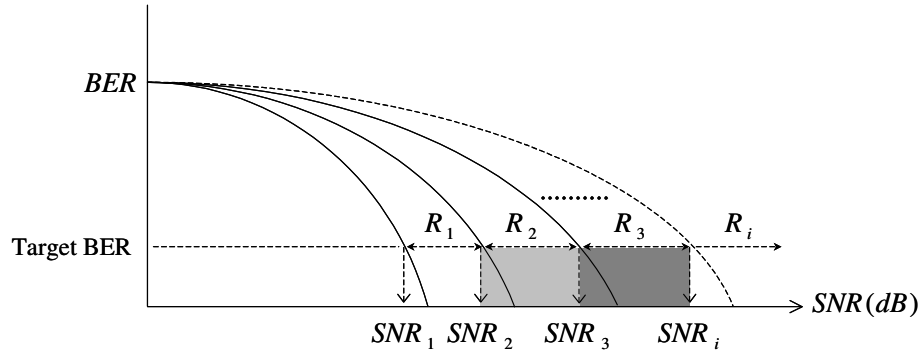
Figure 10. Illustration of the conventional SNR based rate switching.

where SNR_i is the minimum SNR to meet the target BER with the rate R_i. However in DORA, the SNR range for the same transmission rate can be further shifted down to lower SNR range, if the optimal fragmentation improves the goodput such that the same goodput in the conventional rate switching can be obtained by DORA. That is

$$R_{opt} = R_{i\_opt,} \quad SNR'_i \leq SNR < SNR'_{i+1}. \tag{16}$$

where SNR'_i is the minimum SNR to achieve the same goodput for the conventional rate

R_i. Figure 11 illustrates the optimum rate switching in DORA. This rate switching

reduces the energy to be transmitted for the nodes, and increases the overall network

goodput by reducing the interferences adjacent to the nodes.
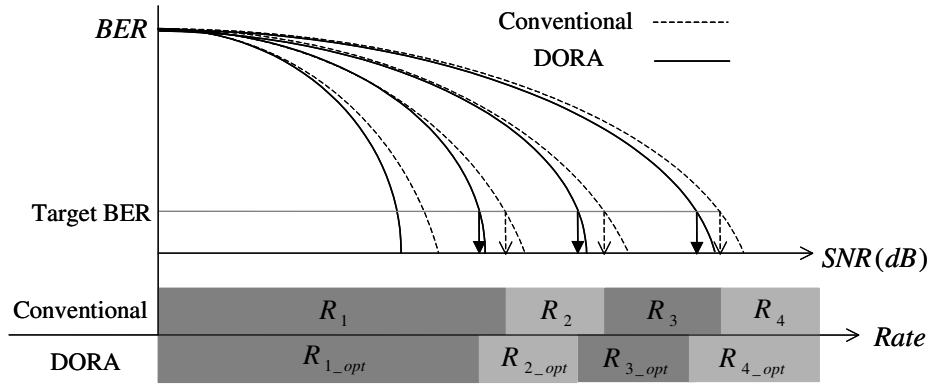
Figure 11. Illustration of SNR based rate switching in DORA.

3.3 Adaptive Channel Estimation

The challenging problem of SNR based rate switching and other approaches that

use SNR of the receiver is to obtain the SNR, which is not supported in the 802.11

CSMA/CA MAC standard. In [5][6] and [14], a modified RTS/CTS exchange is used to

feed back the channel conditions of the receiver, which requires modifications of the

protocol. The link adaptation strategy [11][12] uses the received signal strength (RSS) of

the frame from the access point to select the best transmission rate for the sender. This

approach assumes that the RSS has a linear relationship with the SNR of the receiver.

However, this assumption is not valid when the AP supports multiple rates for downlink

channels. Since mobile nodes may have different network cards, the transmission power

of each user may be different. Therefore, SNR estimation with RSS for each station should be different, and the AP is not able to select proper rates individually for the stations. Furthermore, in the presence of interference at the receivers, strong RSS at the AP does not guarantee better SNR, and each user may experience different profile of interference.

The adaptive estimator in DORA uses on-demand, low overhead UDP messages to
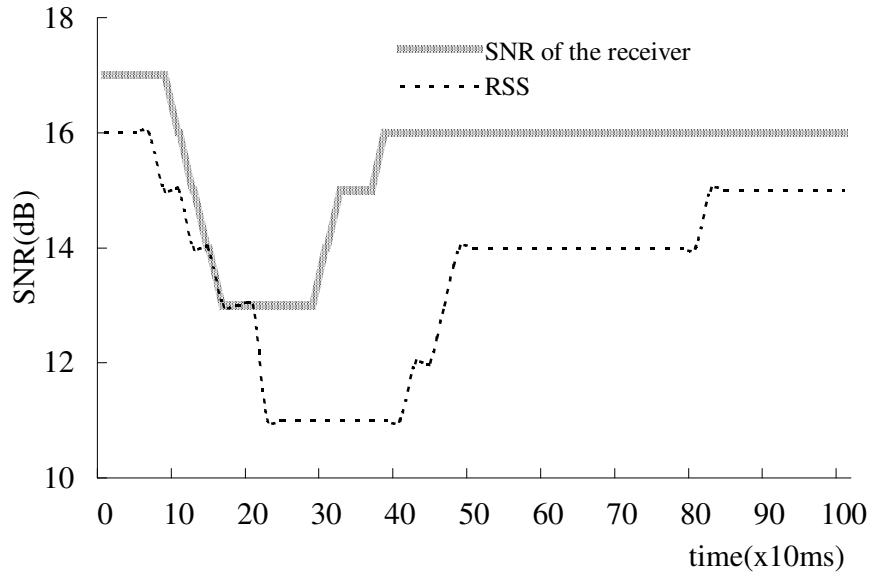
**Figure 12. Measurement of SNR and RSS with Tx power -10dBm
in a typical office environment.**

avoid modification of existing protocols. In the estimator, the received signal strength from the receiver is defined as $y(k)$. Suppose any mobile stations can overhear $y(k)$ as long as they are in the communication range. If the average received signal strength up to $k-1$th frame is denoted as $\bar{y}_{RSS}(k-1)$, and the SNR estimation of the $k+1$th frame is defined as $\hat{y}_{SNR}(k+1)$, the estimation of the SNR at the receiver can be represented as

$$\hat{y}_{SNR}(k+1) = (1-\gamma)\{\alpha\, \bar{y}_{RSS}(k-1) + (1-\alpha)\, y(k)\} + \gamma\, \bar{y}_{SNR}(k). \tag{17}$$

where $\bar{y}_{SNR}(k)$ is the average SNR of the receiver, and $0 \leq \alpha \leq 1$. The term, $\gamma \geq 0$, is to decide how much moving average of the received signal strength will be added to the average SNR of the receiver in the estimation.

Given that the uplink and downlink channels are not always geographically symmetric, the estimation by only using the observed received signal strength is not valid for selecting L_{opt} and R_{opt}, even though there is no interference or hidden terminals at the receiver. In Figure 12, the difference between SNR of the receiver and the RSS at the sender can be observed for the same transmission power of -10dBm with LOS in a typical office environment. Total 50 packets of 1500 bytes MSDU are used to measure the SNR of the receiver and RSS at the sender for the same –95dBm noise power using
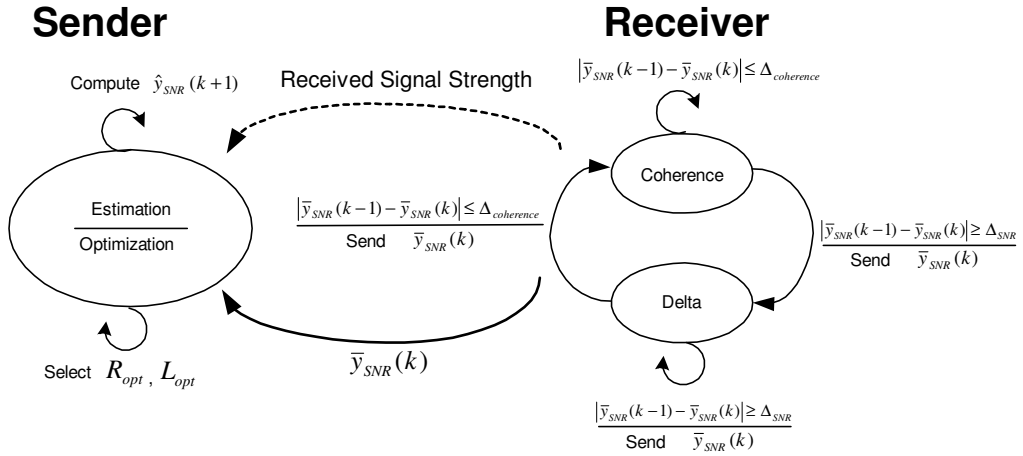
Figure 13. State diagram of the on-demand adaptive estimator in DORA

mad-wifi driver. However, the received signal strength is not totally irrelevant to the SNR of the receiver either. It provides a rough figure of the SNR in different time scale and amplitude in dB. Thus, the adaptation algorithm should be informed of the initial average SNR of the receiver in any forms so that it tracks the SNR while reflecting the variation

of the RSS on it. Details of the estimation algorithm can be implemented using the state diagram illustrated in Figure 13.

To verify the performance of the estimator, real time estimation is executed in Interstate-85 North Exit 99 to 102 in Georgia. The network card is externally connected
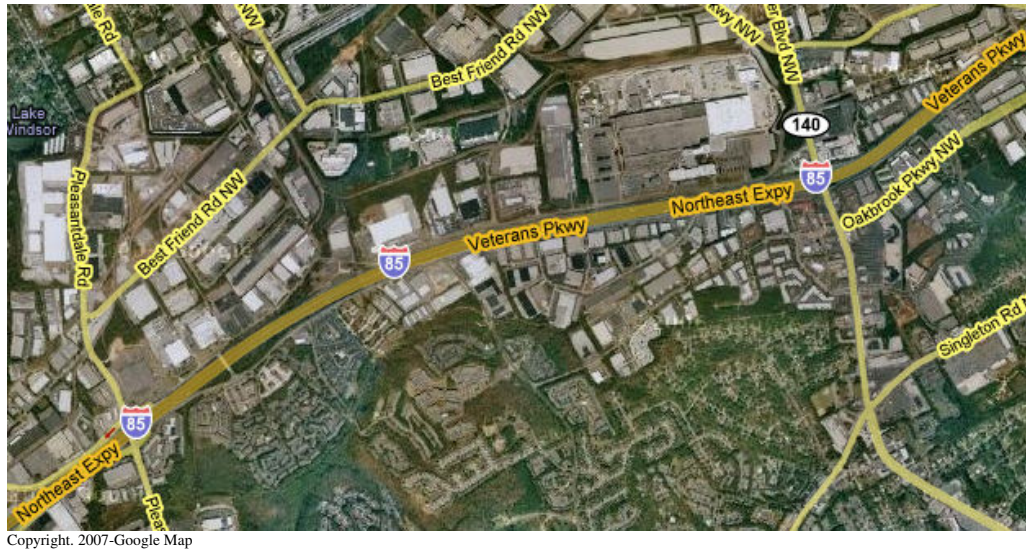
**Figure 14. Interstate-85 North, Georgia, Exit 99 to 102
for the first passing scenario.**

to the antenna, which is placed using magnetic base on the center of the roof in the car. To record exact location and speed of the vehicles during the experiment, GPS antenna with a pocket PC is installed in each vehicle. For the pocket PC, GPS2PDA to download GPS data to store in the PC is installed.

For the estimator in Figure 13, α and γ values are set to 0.9 respectively. How quickly the algorithm tracks the SNR can be determined by choosing the parameters in the equation (17) with Δ_{SNR} and $\Delta_{coherence}$. However, finding optimal α, γ and the other parameters in a typical wireless vehicular-to-vehicular environment is out of the research scope and should be included in future research.

In this experiment, Δ_{SNR} is set to 0.2dB and $\Delta_{coherence}$ is 0.1dB. The SNR and the RSS are sampled in every 10 ms, and the average of 50 samples are used to calculate $\bar{y}_{RSS}(k-1)$ and 20 samples for $\bar{y}_{SNR}(k)$ respectively. The receiver informs the sender of $\bar{y}_{SNR}(k)$ in UDP messages when the difference between the averages is greater than Δ_{SNR} (i.e., $|\bar{y}_{SNR}(k-1)-\bar{y}_{SNR}(k)| \geq \Delta_{SNR}$), or $\bar{y}_{SNR}(k)$ stays longer than the channel coherence time T_c [22], the time duration over which the channel impulse response is essentially invariant. That is

$$T_c = \sqrt{\frac{9}{16\pi f_m{}^2}} = \frac{0.423}{f_m}. \tag{18}$$
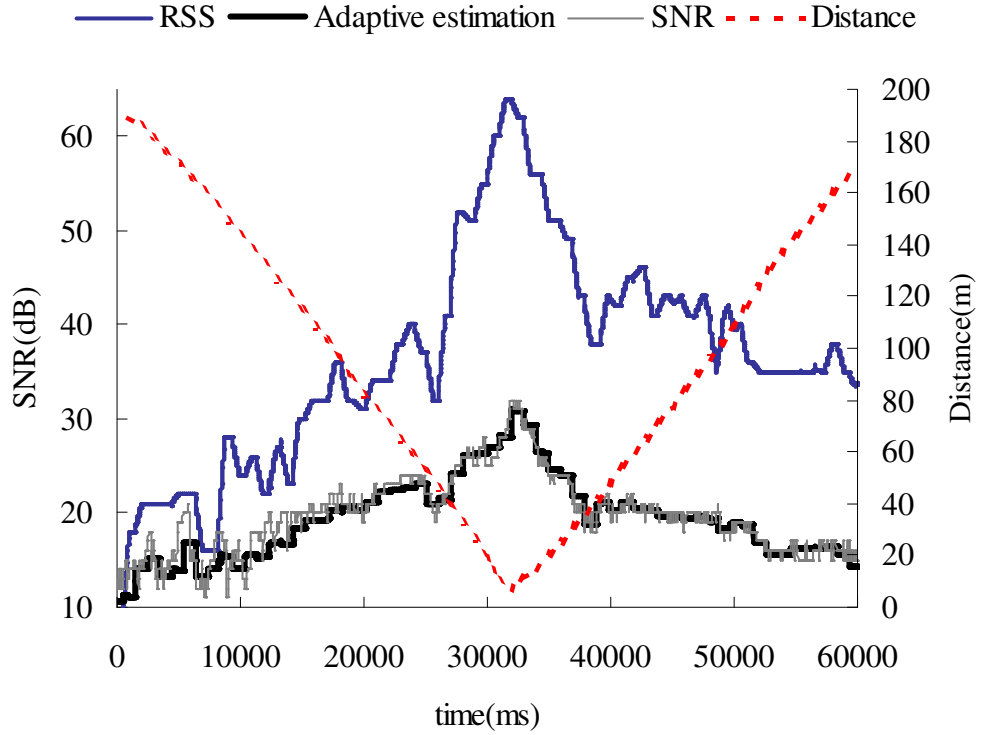
Figure 15. Adaptive channel estimation for the passing scenario in Interstate-85 North, Georgia, Exit 99 to 102.

where f_m is the maximum Doppler shift. T_c may vary with respect to the BER performance of the modulation schemes and f_m. In this experiment, T_c is set to 50 ms.

For the first passing scenario in Figure 15 and Figure 16, the sender in the first lane passes the receiver in the last lane. The initial distance between each vehicle is approximately 200 meters. The transmission power is set to the default power of 17 dBm.
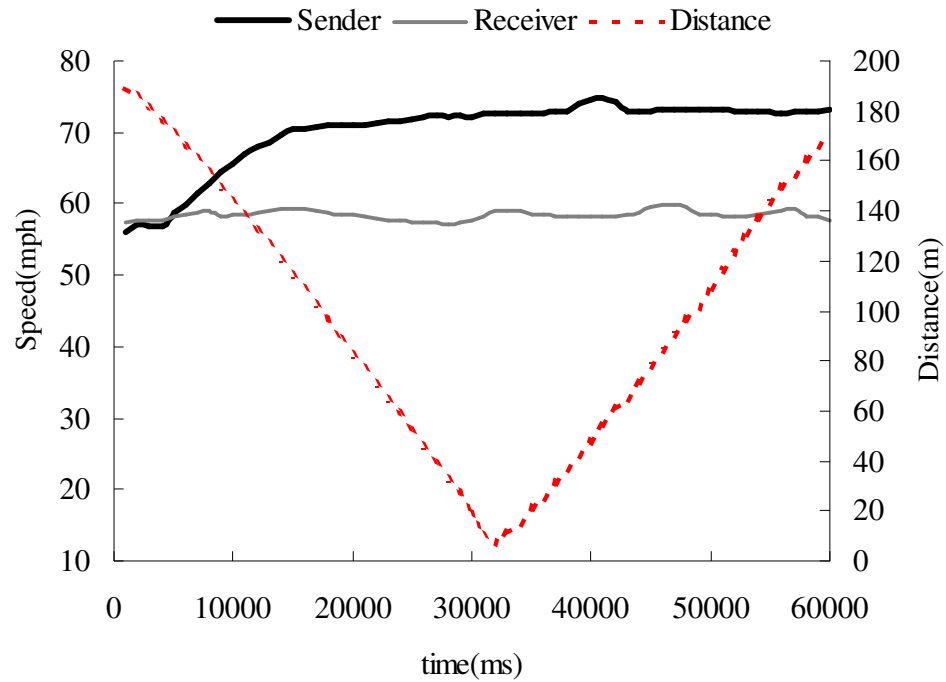
Figure 16. Speed and distance of the vehicles for the passing scenario in Interstate-85 North, Georgia, Exit 99 to 102.

To measure the exact location and the speed of the vehicles, GPS receivers are equipped in each vehicle. The average speed of the receiver is approximately 58.4 mph while the sender passes the receiver with the average speed of 70.4 mph. The channel is saturated by 1500 byte MSDU in TCP connection, and the SNR is measured by pooling iwspy from the driver in every 10 ms. Proxim 802.11b cards with external antennas are used. In Figure 15 and Figure 16, the estimation tracks quite precisely to the SNR of the receiver with only 46 UDP messages in 60 seconds. This is extremely low overhead taking into

consideration of a typical passing scenario in highways with trucks, different curvature and elevation of the road. Normally, just a 2 bytes UDP message is enough to represent the SNR for 0.1dB scale.

For the second scenario, two vehicles cross each other in residential areas. All the parameters in the estimator are the same as the first passing scenario. The average speed of the vehicles is approximately 38 mph in opposite direction. Thus, there is 76 mph speed difference, and this will introduce severe Doppler frequency shift and SNR

Copyright. 2007-Google Map

Figure 17. State street at Atlanta, GA for the second scenario,
crossing vehicles in residential areas.

variation compared to the previous experiment. The estimation results are depicted in Figure 18 and Figure 19. The peak SNR of the channel reaches approximately 30 dB when the two vehicles are crossing each other, and it is roughly the same as the previous passing scenario. However, the time duration that may ensure reliable connection between the vehicles is much shorter than the previous passing scenario. For example, the time interval that the SNR exceeds 20 dB for the crossing scenario in residential areas is

just 20% of the passing scenario in Interstate highways. Thus, crossing vehicle-to-vehicle communication in Interstate highways is much more susceptible to the link failure, and it produces challenging routing problems to be solved in a short time.

Even though, the SNR varies severely in this channel, the estimation overhead produced by the on-demand UDP messages in the estimator yields less than a two-byte message in a second. These UDP messages, nevertheless, can still influence the system goodput, and sacrifice bandwidth in the network. In Figure 20, the influence of the UDP messages on the system goodput is described. Each vehicle transmits UDP control messages to estimate the SNR of the receiver during the TCP transmission with 1500 bytes MSDU for 4% of packet error rate in NS-2 simulator. Even in the worst situation of
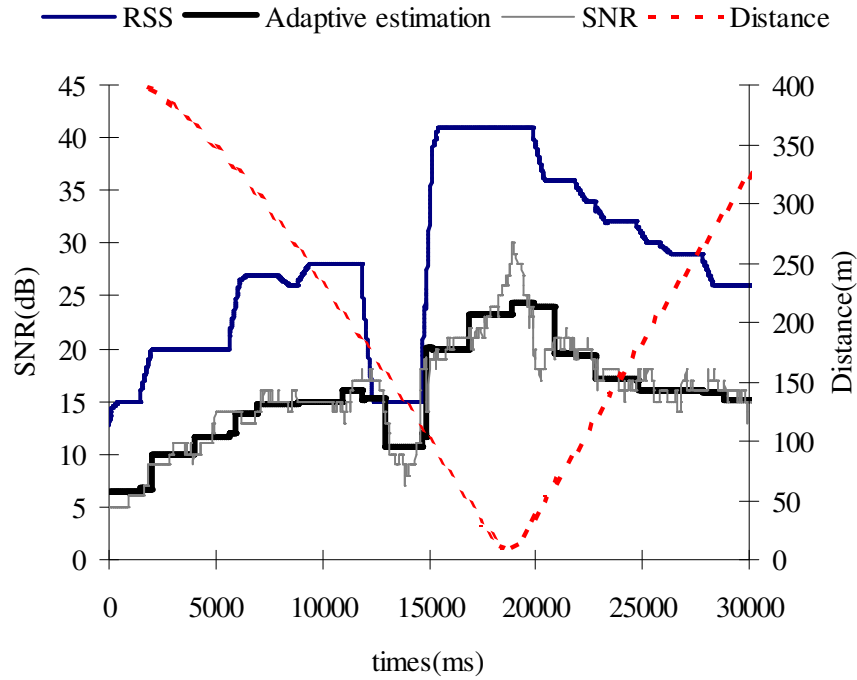
Figure 18. Adaptive channel estimation for the crossing scenario in residential area, State st. NW, Atlanta, Georgia.

30 users with one UDP messages in a second, the performance loss is less than 1.6% compared to the normalized goodput of the basic operation, while RTS/CTS based

channel estimation in [5, 6] and [14] introduces 11% of the loss. Further overhead reduction can be made by adjusting parameters in equation (17), if a coarse estimation is more desirable by sacrificing the accuracy in certain circumstances. In most cases, the average of less than one UDP messages per second can be obtained in the vehicle-to-vehicle communication by using the on-demand UDP estimator.
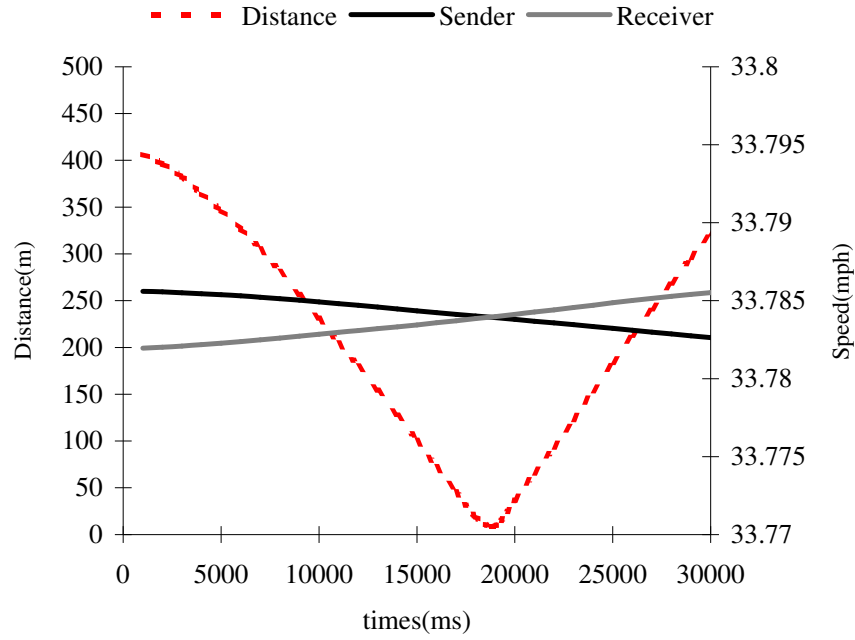
Figure 19. Speed and distance for the crossing scenario in residential area, State st. NW, Atlanta, Georgia.

Nevertheless, the total performance gain that DORA achieves is greater than basic operation as described earlier in Figure 4.

3.4 Other Considerations

The SNR of the receiver is one of the most important components in the calculation of L_{opt} and R_{opt}. DORA uses on-demand adaptive estimator instead of using an explicit SNR feedback as in [5, 6, 14] to decide optimum values in the channel. Note

that the target bit error rate or symbol error rate in SNR based rate switching are fixed. If the SNR fluctuates severely such that the BER also changes dramatically, the optimum rate adaptation automatically switches the transmission rate to a higher or lower rate in order to maintain the target BER or SER. Furthermore, selecting wrong optimal fragmentations are unlikely as the estimation algorithm has a very low approximation error (e.g., average 0.373 dB for 6,000 samples in the previous experiment, Figure 15). For example, assume 750 bytes of optimal MPDU for 15 mobiles at the BER of 1×10^{-5} in Figure 6. To select 500 bytes due to the channel estimation error, which is the optimal
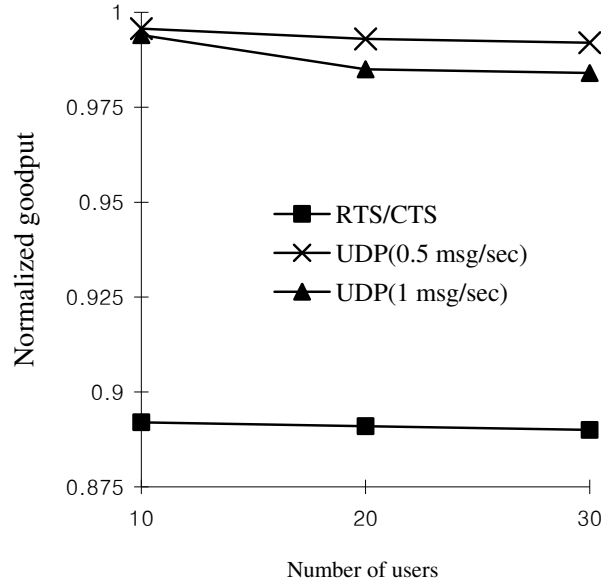
Figure 20. Adaptive on-demand UDP message and RTS/CTS overhead.

value for the channel 3×10^{-5}, at least 1.1dB of SNR estimation error is required. However, 500 bytes MPDUs still achieve 99.98% of the goodput against the optimal value, 750 bytes. In case the optimal fragmentation selects 1500 bytes, it would transmit larger frames in a bad channel, and it loses 9% of goodput. However, that is unlikely to occur in the proposed adaptive estimator, since the estimator would need to have an error of at least 4.61 dB.

In the non-linear system given by (13), senders must determine L_{opt} and R_{opt}. Obtaining R_{opt} is straightforward if the senders can estimate the SNR precisely for a given target BER or SER. However, solving (13) to get L_{opt} in real-time is a computationally expensive task. By incorporating the knowledge that L_{opt} is a divisor of the original packet length, further simplification can be made to alleviate the complexity of the system for the real time implementation. For example, if the packet is 1500 bytes, the valid candidates of L_{opt} are 1500, 750, 500, and 300 bytes in Figure 7. This enables the system to use a small, efficient lookup table to determine L_{opt}. Further reduction can be made to decrease the complexity of the system without performance degradation by setting a minimal packet length considered for fragmentation. In DORA implementation, 300 bytes MPDU is the minimum frame length, and any frames less than 600 bytes will not be considered for fragmentation.

For network security, it is the sender that computes L_{opt} and R_{opt}. Thus, if associated receivers are trusted entities, it would not introduce security problems. Additionally, senders could be any of the wireless stations, i.e., client stations and access points in WLAN, or wireless mobile stations in a multi-hop ad hoc networks and vehicle-to-vehicle networks.

CHAPTER 4

DORA IN WLAN

The IEEE 802.11b/g [1, 3] technologies are one of the most widely deployed wireless lan technologies. Many people are using the Internet more than ever and the demand for broadband wireless access is increasing rapidly. By using unlicensed 2.4GHz ISM spectrum with simple design, the cost of the networks is fairly lower than 3G networks. However, WLAN covers only a few hundred meters and mobile users are unable to make connections when moving to other networks in WLAN. Users in the future are expected to use both types of networks, one for wide coverage and reliable seamless connection, and the other for cheap and high data rate.

The IEEE 802.11b [1] operates in two different physical radio units. One is Infra red Unit, and the other is spread spectrum unit. Direct Sequence Spread Spectrum (DSSS) physical layer techniques is dominantly used in general for university access networks, hotspots such as train stations, hotels, coffee shop and airports. Nevertheless, actual data rates are far less than theoretical maximum throughput, and heavily dependent on the network configurations and the quality of the channel. Therefore monitoring and configuring the parameters are a very important job for network managers to achieve maximum available throughput.

Using SNMP protocol with the standard dot11 MIB module, the configurations of access point in WLAN can be monitored and managed by network administrators. To change the configurations of the network cards, iwconfig can be used to configure transmission power, frequency of the channel, fragmentation threshold, transmission rates

and so on. In this section, the performance benefit of DORA by using the optimal fragmentation technique in WLAN is presented with experimental results.

4.1 Configuration of the Experiment

To evaluate the performance of DORA in CSMA/CA MAC, extensive experiments are executed in WLAN. Note that the optimum rate R_{opt} in DORA can be determined with the on-demand estimator in the previous section 3.3 for a given target
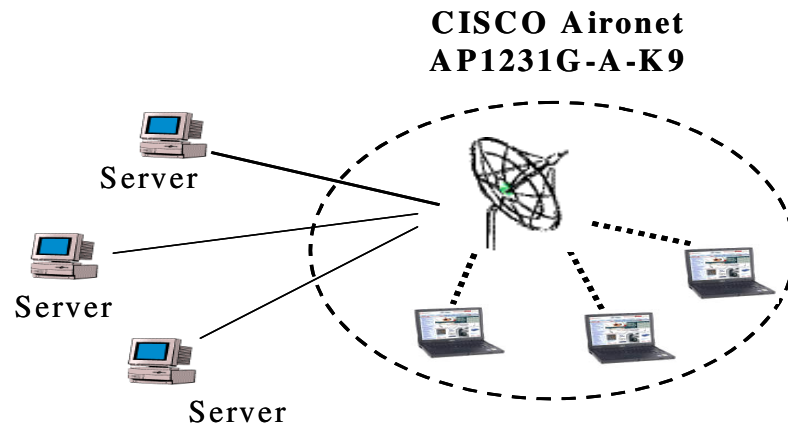
Figure 21. WLAN experiment topology.

BER or SER. Thus, to obtain more accurate L_{opt} in goodput measurements, ARF [4] built in Proxim network cards is disabled to fix the rate to 1 Mbps. Figure 21 shows the experimental topology setup. For the access point, CISCO Aironet 1231-G-A-K9 [23] access point is used with default configuration as shown in Figure 22. Three Linux mobile stations in Figure 23 and servers are used in an office environment. Each server establishes a TCP flow to the one of the clients and transmits an average of 30 packets with poison distributed inter-departure. The size of the MSDU is 1500 bytes, and three

TCP flows through the access point to the stations saturate the wireless link for the maximum throughput, 1 Mbps, in DBPSK IEEE 802.11b PHY modes. Then, fragmentation thresholds are configured to slice the 1500 bytes MSDU into MPDUs to find L_{opt}.

Figure 22. CISCO Aironet 1231-G-A-K9 in WLAN experiment.

For each fragmentation threshold, 20 trials of 100 seconds per trial are made for MPDUs of 300 through 1500 in 10 bytes increments in each given BER. To estimate the BER with the measured SNR, the BER equations found in [19] for an additive white Gaussian noise channel is used. The AWGN channel model is not realistic in WLAN, but this model is useful for reference purposes, since no exact channel model for the experiment is available. For DBPSK,

$$P_{DBPSK} = \frac{1}{2} e^{-E_b / N_0}, \tag{19}$$

where E_b / N_0 is the SNR per bit.

For the first experiment in WLAN, three stations are placed at 'A' in Figure 24 such that the average SNR of each receiver exceeds 15.42 dB to accomplish bit error rate

Figure 23. Three laptops for WLAN experiment.
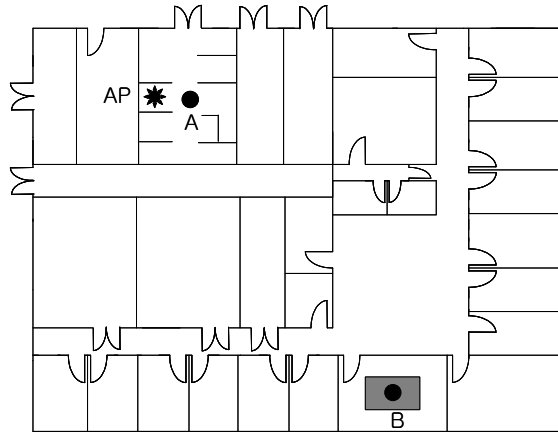
Figure 24. An indoor office for the experiment in WLAN.

of 10^{-7} in equation (19). In addition, the second experiment at point 'B' in the Figure 24 is set up to have an average 10.491 dB with standard deviation of 1.348 dB, which corresponds to a BER of 1.4×10^{-5} for a typical office environment.

4.2 Performance Evaluation in WLAN

The experiment results in Figure 25 show the overhead of the fragmentation, and the fact that different MPUDs can change system goodput dramatically. For comparison with the numerical results, a reference curve of 10^{-7} for the perfect office environment is drawn with the experimental result at the position 'A'. In the second experiment, the reference curve of 3×10^{-5} is drawn, which has an offset of 0.8 dB from the average SNR of 10.491 dB at the point, 'B'. This SNR offset is reasonable if the vulnerability of the low SNR channel against interference is considered in the office environment verses the ideal AWGN channel model in (19).

For the first channel at 'A' in the figure, the fragmentation threshold should be 1500 bytes MSDU plus 28 bytes of MAC header, and 8 bytes of sub-network access
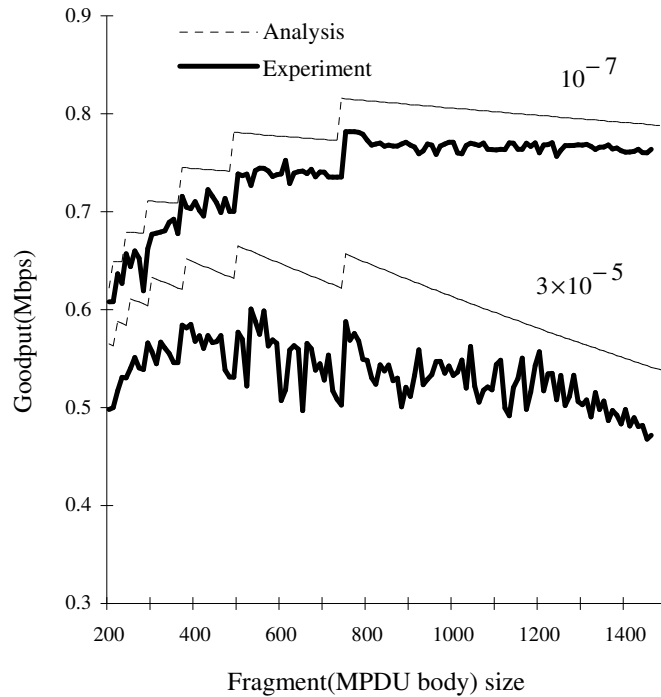
Figure 25. Goodput vs. MPDU in WLAN.

protocol (SNAP) header. It is interesting to see the second peak of the goodput at 750 bytes MPDU for the first channel. If the 1500 bytes MSDU is divided into 760 bytes, a slightly larger fragment that is more vulnerable to random errors sacrifices the same overhead as 750 bytes. Likewise, for 740 bytes, although a shorter fragment is robust against random errors, one more overhead of $H + 2SIFS + ACK$ is introduced, and this overhead has more influence on the goodput than the random errors.

For the second curve of BER 3×10^{-5}, the maximum goodput is realized by the 500 bytes MPDU, and the optimal fragmentation threshold value should be 528 bytes
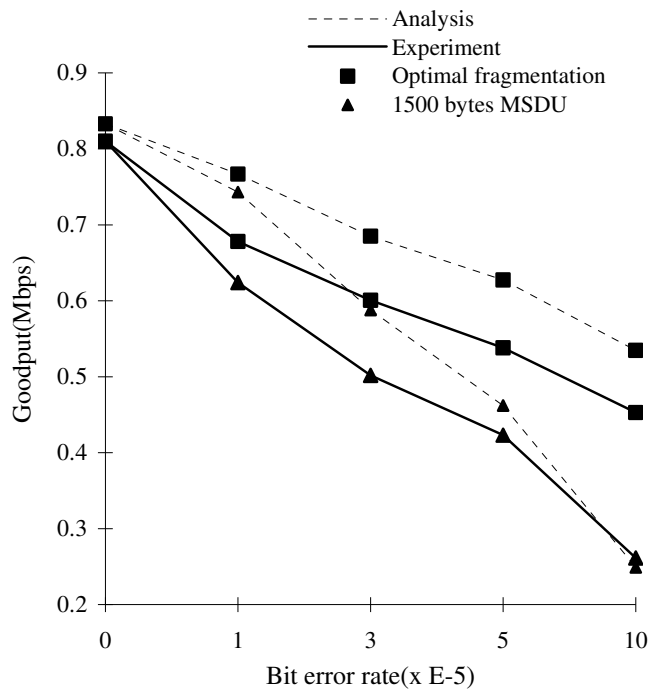
Figure 26. Goodput vs. bit error rates in WLAN.

taking into consideration of the 28 bytes of the MAC header. An additional 8 bytes of SNAP header are required in the last fragment. Thus, the threshold for the MSDU is three 531 bytes MPDUs that carry 3 additional bytes for the SNAP header in each fragment.

The total packet to transmit to the air is 555 bytes, which includes 24 bytes of physical-layer convergence protocol header and preamble.

The experiment shows that packet loss is a major obstacle achieving higher goodput in a bad BER channel, and a smaller fragment has more benefit than the drawback of the overhead in the channel. From a moderate BER of 1×10^{-5} to 5×10^{-5} in Figure 26, approximately 18.4% improvement of the average goodput can be achieved. In a situation where the channel becomes worse, for example, at BER of 10×10^{-5}, a 73% significant improvement in goodput is obtained in this experiment.

Given number of stations and BER in (13), the optimal fragmentation threshold that maximizes the goodput is uniquely determined. By choosing these optimal values, the maximum goodput can be obtained by using DORA. Since the 802.11 standard mandates all receivers support fragmentation, this optimal fragmentation in DORA can be applied to any variable sized packets with the optimum transmission rates.

CHAPTER 5

DORA IN AD HOC NETWORKS

Ad hoc is a network that requires no infra suructure to form connections to transmit data among the nodes in the network. The stations within range can discover each other to form routing path by flooding or forwarding information to the other nodes. Thus, the network connections can be extended to multiple nodes to transport data through the routing path dynamically. If the nodes in the routing path move to the outside of the network, a new routing path is established to maintain connections using routing algorithms. These types of networks are very efficient especially in battlefields and other places where no central coordinators are available. However, it is very fragile network compared to wired networks due to high mobility and dynamical network environment in general.

DORA is a CSMA/CA based MAC layer technique. Thus, without losing generality, DORA can be applied to ad hoc networks that use the same MAC protocol.

5.1 Configuration of the Experiment

Figure 27 describes the topology of the experiment consisting of four mobile computers equipped with 802.11b network cards. To reduce the dependency of results depending on ad hoc routing protocols and overheads, a static forwarding routing table is configured through the routing path from the sender to the receiver at the last hop.

In order to see the maximum achievable goodput in a perfect channel, the nodes are placed such that the average SNR of each link is 21.3dB. The SNR exceeds approximately 6 dB more than the bit error rate channel of 10^{-7} in equation (19). Each node has the transmission power of 20 dBm, and links between each adjacent station has 85dB path loss. The sender generates 1500 bytes of MSDU, and establishes a TCP flow to the receiver through the wireless nodes in the ad hoc routing path. With poisson-distributed inter-departure, the sender transmits 60 packets per second on average to the
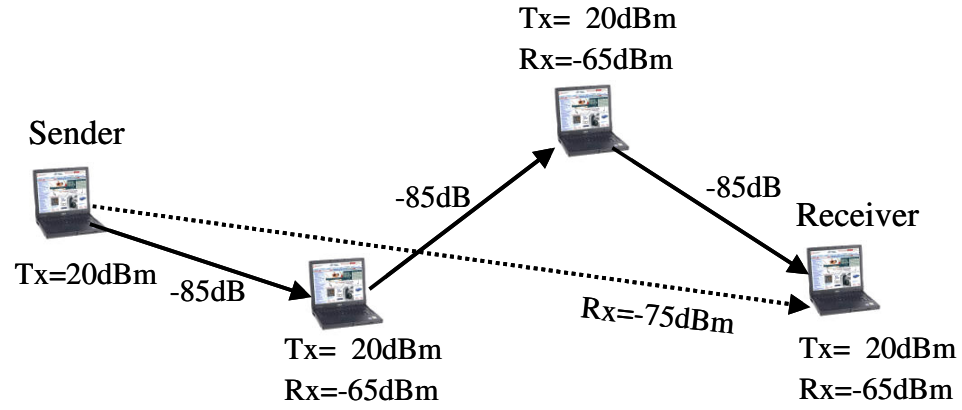
Figure 27. Multi-hop Ad hoc topology for BER, E-7.

receiver, which is enough to saturate a three-hop ad hoc network. Then, the 1500 bytes MSDU are fragmented into MPDUs to find the optimum fragment, L_{opt}. For each fragmentation threshold, 20 trials of 50 seconds per trial are executed for MPDUs of 300 through 1500 bytes in each given BER. The same BER equations found in [19] is used as in the previous WLAN experiment. In addition, to explore the performance of DORA in a typical wireless channel, the transmission power in the second experiment is reduced to

41

10dBm with the same topology configurations. This yields an average SNR of 11.1dB, which has an offset of 0.3 dB from the BER channel of 10^{-5} in (19).

5.2 Performance Evaluation in Ad Hoc Networks

The results in Figure 28 clearly show two distinct performance differences between the channels. Contrary to the previous results in WLAN, the average goodput for each MPDU in a perfect channel is lower than the one in a typical channel by 91.3kbps for 1 Mbps DBPSK modulation. The rationale of the fact is that by increasing SNR between links, the random packet drops can be reduced. However, strong signals introduce severe interference to the adjacent links, and prohibit the other stations in the
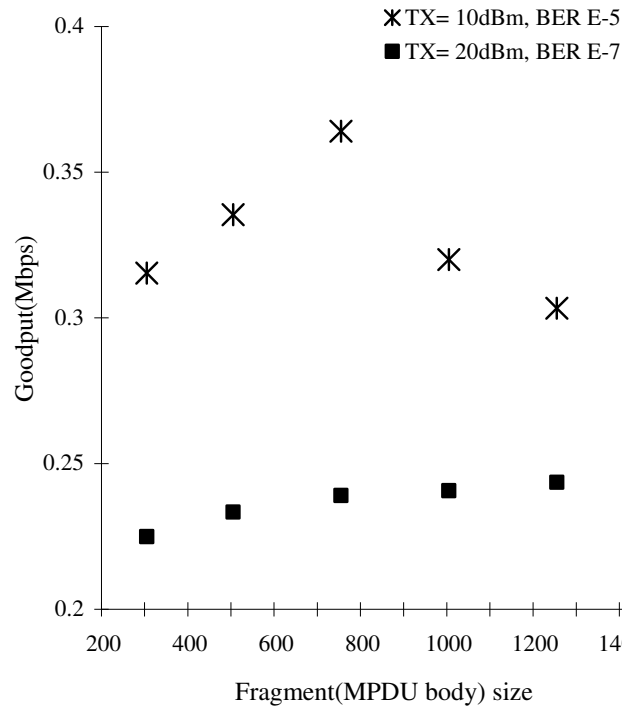
Figure 28. Goodput vs. MPDU in a three-hop ad hoc network experiment.

routing path from routing the packets at the same time.

Note that the analytical model (13) considers one-hop link goodput of CSMA/CA. The number of end-to-end hops in ad hoc networks has a direct impact on the goodput. Consider TCP at a steady state with no queuing and processing delay. The end-to-end throughput of the multi-hop string topology is inversely proportional to the round trip
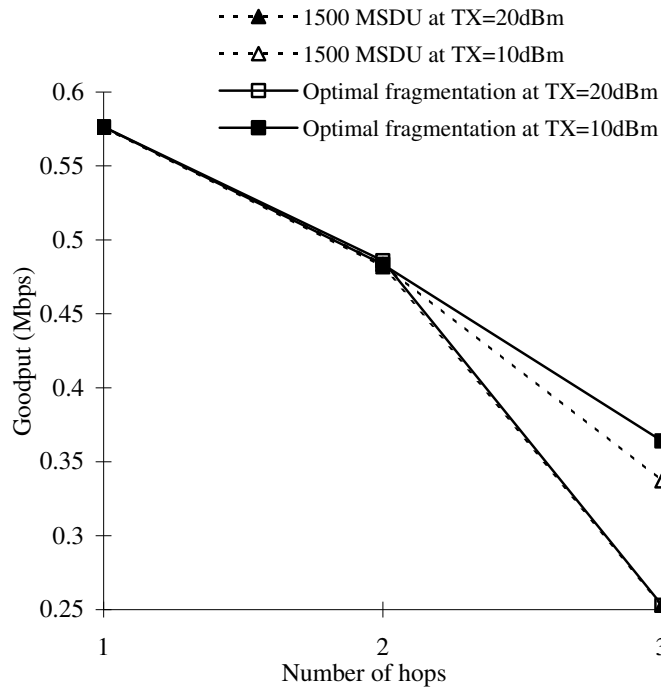
Figure 29. Goodput vs. number of hops in ad hoc networks.

time (RTT). For the perfect channel in Figure 27, the signal power of each node is strong enough to prevent other nodes from routing packets. Therefore, the RTT will be roughly three times larger for a three-hop string ad hoc network, and goodput drops to approximately the one third compared to that of the one-hop link. However, by reducing the transmission power to 10 dBm for the BER channel of 10^{-5}, when the first node transmits to the second node, the fourth node can simultaneously transmit packets to the

third node. Similarly, the second node can transmit to the first node while the third node is sending packets to the forth node. Thus, the effective RTT is two times larger than the one-hop link, and the goodput drops to half of the analytical one-hop model (13). A general analysis of TCP throughput in the IEEE 802.11 multi-hop ad hoc network can be found in [24].

Numerical reference curves for a three-hop ad hoc network are drawn with the experiment results in Figure 30. This shows that proper selection of the routing path is important in ad hoc networks to improve goodput, and DORA performs better in this low SNR channel. As a result, DORA accomplishes 48.1% of goodput enhancement, and provides a more energy efficient routing algorithm with less transmission power. Further
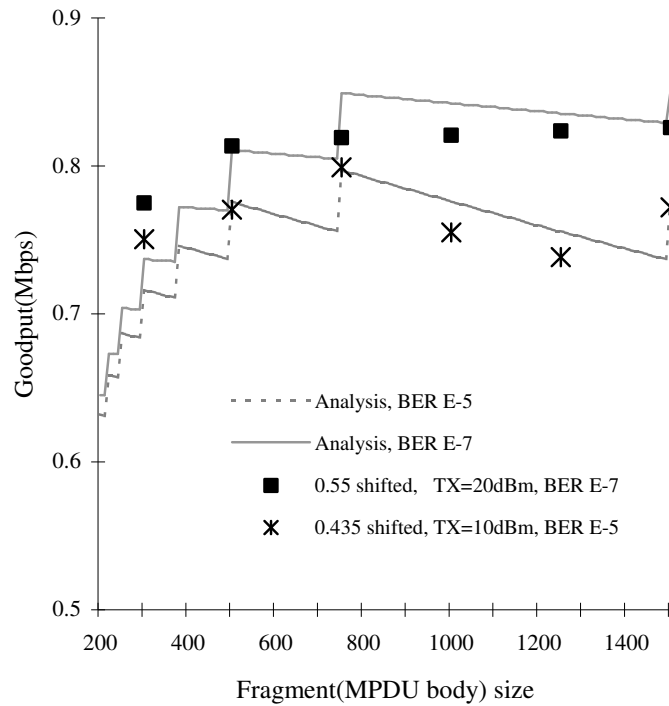
Figure 30. Shifted goodput vs. MPDU in a three-hop ad hoc network experiment.

research can be performed to find optimal routing path over wireless ad hoc networks to maximize goodput using DORA. Note that DORA is to optimize one-hop wireless link rather than end-to-end routing path, and it provides maximum achievable goodput of each link for the established routing path. However, this path may not be the best route in terms of maximum goodput. Therefore, finding the best routing path that incorporates individual optimized links to the last-hop is a challenging problem due to difficulty of exhaustive search for the possible routing paths among many nodes in dynamic mobile ad hoc networks. An analysis of end-to-end performance along the optimized links in ad hoc networks with TCP interaction can be considered for future research as well.

CHAPTER 6

DORA IN VEHICLE-TO-VEHICLE NETWORKS

Various vehicular communication technologies have been proposed to provide seamless wireless communications. Third generation networks support wide coverage, seamless mobility, and quality of service for mobile users. However, these connection-oriented networks require expensive infrastructure for deployment, and they are effective mostly in voice traffic applications. Short-range vehicular communications can be established using IEEE 802.11p [25], specifically Wireless Access in Vehicular Environments (WAVE) for the Dedicated Short Range Communications (DSRC). These technologies are efficient to exchange data between vehicles or vehicles to road side in the licensed 5.9 GHz band. Since the range of these protocols can be extended using mobile multi-hop ad hoc networks discussed in the previous section, it is important to adapt the physical and MAC layer properties to complete data transaction in very short time for high-speed vehicle communications.
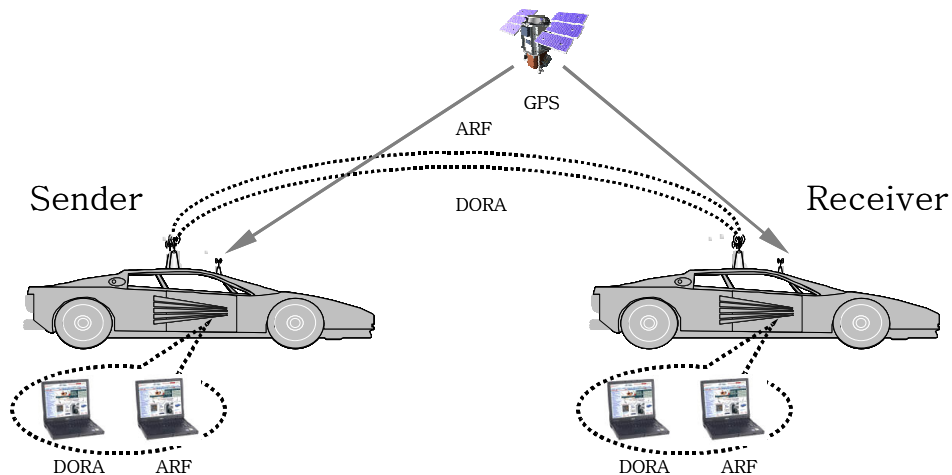
Figure 31. Illustration of Vehicle-to-Vehicle Experiment.

Table 1: External antenna specifications.

Frequency	2400-2500 MHz
Gain	5 dBi
Impedance	50 Ohm
Maximum Input Power	100 W
Weight	< 0.5 lbs with base
Length	10 inch including base
Mounting	Magnetic
Operating Temperature	-40° C to 85° C
Polarization	Vertical
Wind Survival	> 200 MPH

6.1 Configuration of the Experiment

Figure 31 illustrates vehicle-to-vehicle mobile experiment consisting of four
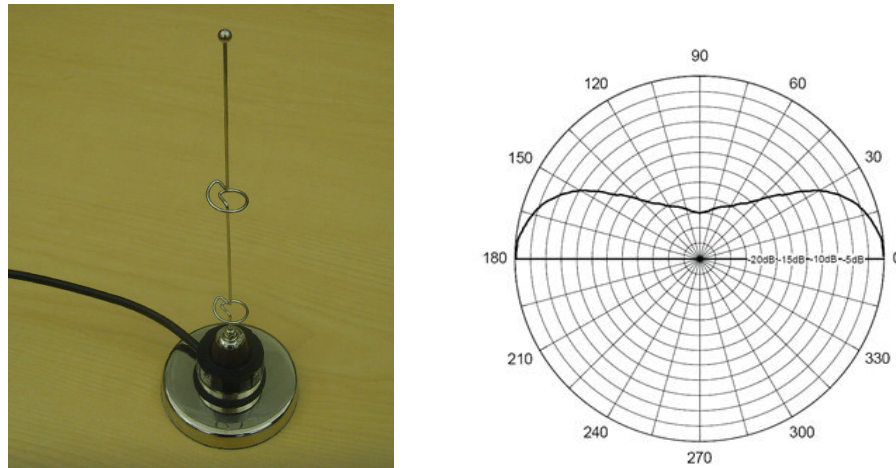
Figure 32. External antenna and vertical radiation pattern.

mobile stations equipped with 802.11b network cards. The network card is externally

connected to the antenna shown in Figure 32. The antennas are placed using magnetic

base on the center of the roof in the car, and separated approximately 1 meter with each

other. Detailed specifications of the antenna are shown in Table 1. To record exact

location and speed of the vehicles during the experiment, GPS antenna (HAiCom HI-303E) [26] with HP iPAQ pocket PC is installed in each vehicle. In Table 2, the specifications of the GPS antenna are described. In HP iPAQ pocket PC, the software (GPS2PDA [27]) to download GPS data to store in the iPAQ pocket PC is installed. Additionally, in order to transfer GPS stored data in the pocket PC to a personal computer in Microsoft Excel spread sheet, *PC-Travel for Windows* [28] is installed to synchronize the PC and the personal computer. The GPS antenna and iPAQ pocket PC are shown in Figure 33. To supply power for the two mobile nodes and the GPS device in each vehicle, 200-Watts power inverter is used with a UPS. These are all the same equipments used to experiment the adaptive channel estimation between two vehicles in the previous section 3. 3.

For the mobile stations, Ubuntu 6.10 [29] operating system is installed with mad-wifi driver. Mad-wifi driver supports the network configuration of the mobiles and provide SNR, received signal strength, and data received through the network interface. All four mobile stations are configured to transmit in the same cell and channel to cause collisions in the network. To estimate the SNR of the receiver using on-demand adaptive

Table 2: HAiCOM HI-303E GPS receiver specifications.

Channels	12
Position Accuracy	25m CEP without SA
Voltage	DC 3.3V +/- 10 %
Satellite Reacquisition Time Accuracy	100 ms
Protocol	NIME V2.2, 4800, N, 1
Maximum Altitude	18,000m
Maximum Velocity	514 m/s
Maximum Update Rate	1 Hz
Weight	< 60 g
Operating Temperature	0° C to 60° C

Figure 33. GPS antenna and iPAQ pocket PC.

estimator in DORA, the average SNR and received signal strength of the receiver are required at the sender. The SNR is sampled in every 10 ms using iwspy with perl script at the receiver, and transmitted to the sender when Δ_{SNR} and $\Delta_{coherence}$ meet the requirements of the adaptation algorithm described in Figure 13. For the received signal strength from the receiver, the sender can overhear it as long as they are in the communication range. Default transmission power of the card, 17 dBm is used for the communication between the sender and the receiver.

For the performance evaluation of DORA in Vehicle-to-Vehicle communication, auto rate fallback (ARF) protocol [4] is used to compare goodput against DORA. ARF is a default rate adaptation algorithm implemented in the card. The algorithm selects the transmission rate of the sender automatically based on how many consecutive successful transmissions have been received. This scheme has inherent limitation to better suit time varying nature of the channels.

For DORA, the on-demand adaptive channel estimator, rate adaptation, and optimal fragmentation algorithms are implemented at the sender and receiver. Therefore, in the vehicle for the senders, DORA and ARF senders are positioned on the passenger side with two separated external antennas on the roof of the vehicle. At the receiver side, DORA and ARF receivers are placed with the external antennas as well.

Each sender generates 1500 bytes of MSDU using netcat, and establishs a TCP flow to the receiver thorough a one-hop ad hoc routing path. Netcat is a simple unix
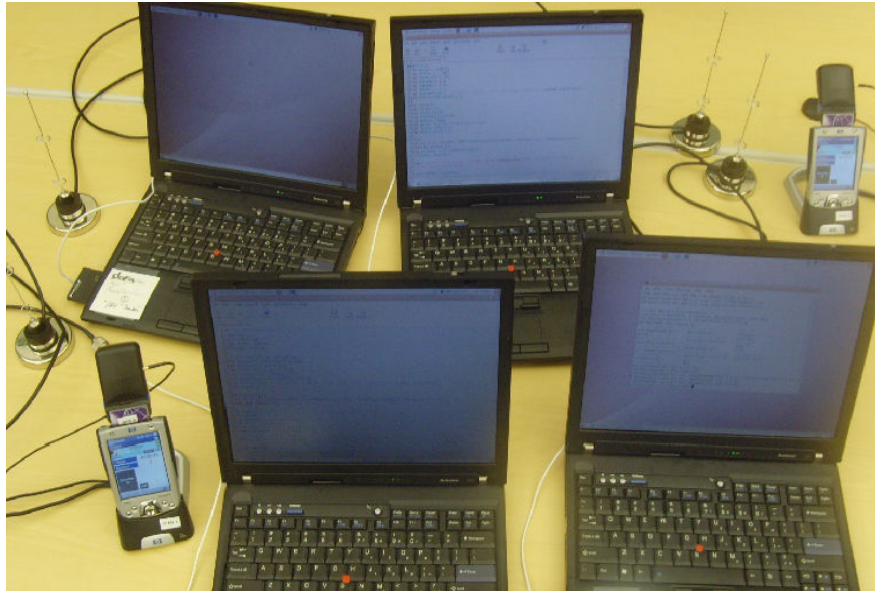
Figure 34. Four mobile stations and GPS used in Vehicle-to-Vehicle experiment.

command that reads and writes date across network connections. Four mobile stations and GPS in Vehicle-to-Vehicle experiment are shown in Figure 34.

6.2 Performance Evaluation in Vehicle-to-Vehicle Networks

For the performance comparison between DORA and ARF, extensive experiments are executed in Interstate-85 North Exit 89 to 102 in Georgia. For the

Table 3: DORA rate switching and optimal fragmentation selection.

SNR > 21.8dB	11Mbps, 1500 bytes
19.3 dB < SNR ≤ 21.8 dB	11Mbps, 750 bytes
18.6dB < SNR ≤ 19.3 dB	5.5Mbps, 1500 bytes
18.1dB< SNR ≤ 18.6dB	5.5Mbps, 750 bytes
17.9dB< SNR ≤ 18.1dB	5.5Mbps, 500 bytes
15.9dB < SNR ≤ 17.9dB	5.5Mbps, 300 bytes
14.9dB< SNR ≤ 15.9dB	2Mbps, 1500 bytes
14.3dB< SNR ≤ 14.9dB	2Mbps, 750 bytes
14.0dB < SNR ≤ 14.3dB	2Mbps, 500 bytes
13.8dB< SNR ≤ 14.0dB	2Mbps, 300 bytes
12.2dB < SNR ≤ 13.8dB	1Mbps, 1500 bytes
10.0dB < SNR ≤ 12.2dB	1Mbps, 750 bytes
9.25dB< SNR ≤ 10.0dB	1Mbps, 500 bytes
8.50dB< SNR ≤ 9.25dB	1Mbps, 300 bytes

estimator in Figure 13, α and γ are set to 0.9 respectively. The estimation parameter Δ_{SNR} is set to 0.2dB, and $\Delta_{coherence}$ is 0.1dB. The SNR and the RSS are sampled in every 10 ms, and the average of 50 samples are used to calculate $\bar{y}_{RSS}(k-1)$ and 20 samples for $\bar{y}_{SNR}(k)$ respectively.

In Table 3, DORA rate switching R_{opt} and optimal fragmentation L_{opt} are shown. As different modulation schemes support different rates, rates can be adjusted to improve network goodput by switching to a higher modulation if channel conditions improve. The BER of DBPSK over an additive white Gaussian noise channel in equation (19) is used to decide R_{opt} and L_{opt}. The approximated SER of DQPSK found in [20] is given by

$$SER \le 2Q\left(\sqrt{\frac{E_s}{N_0}}\right) \quad , \tag{20}$$

where E_s/N_0 is the SNR per symbol. The CCK is a variation of M-ary biorthogonal keying (MBOK) modulation for 5.5 and 11 Mbps, and the SER curve can be found in [21]. Based on these approximated SER, R_{opt} and L_{opt} can be determined using equation (13) and (16) such that the system goodput is always maximum over the entire range of

the SNR. However, the R_{opt} is different from the conventional rate switching. For example, assume the target packet error rate is 8% as described in the standard. When the SNR of the channel improves, conventional rate switching algorithms change the rate from 1 Mbps to 2 Mbps at 18.87 dB to maintain the packet error rate below 8%, which corresponds to the SER of 1.4×10^{-5} in 2 Mbps. The maximum goodput of 1 Mbps is 0.833 Mbps up to the SNR of 18.87 dB. In DORA, however, L_{opt} of 300 bytes at 2 Mbps yields 0.968 Mbps with the symbol error rate of 2×10^{-4} at 13.8 dB. Therefore, DORA can switch the rate to 2 Mbps at 13.8 dB to accomplish 0.968 Mbps, which is 16.2 %

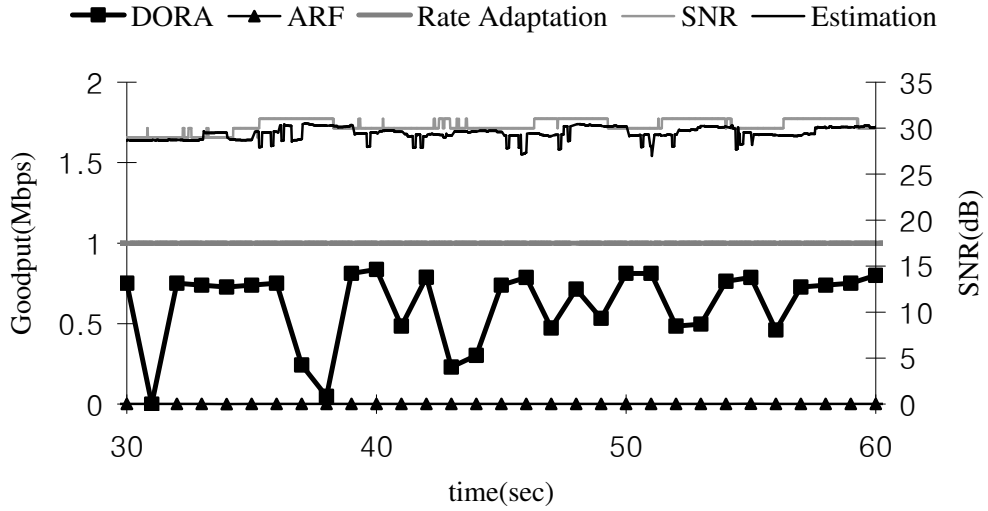**Figure 35. Illustration of low SNR channel performance in DORA and ARF.**

greater than the maximum goodput 0.833 Mbps at 1 Mbps rate. This rate switching provides an energy efficient technique with low battery power obtaining higher data transmission rate.

For the first scenario, the SNR is dropped to a lower SNR after establishing connections between the two vehicles. In the theoretical analysis [19, 20, 21], if the SNR

is 30 dB, the channel is excellent to transmit and receive data without packet drops. However, mobile environments where cars and trucks are driving highways approximately 60 mph with different curvature and elevation of the road are very different from the ideal AWGN channel. Therefore, the actual SNR scale for the mobile communication has big difference from the reference model [19, 20, 21], and adjustment is inevitable to make connections. From the observation obtained in the previous
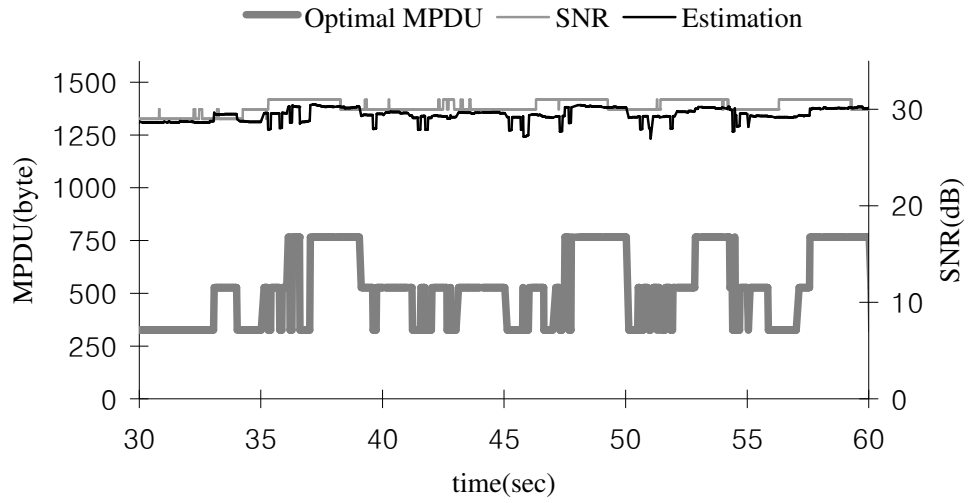
Figure 36. Adaptive channel adaptation and optimal MPDU selection in DORA.

experiments, 30dB is a marginal SNR for the mobile communications to exchange data in 85 South, EXIT 89 to 93. Thus, in the experiment in Figure 35 and Figure 36, on-demand estimator subtracts 20 dB such that actual 30dB SNR is regarded as 10 dB in the Table 3 for choosing L_{opt} and R_{opt}.

To experiment this scenario, the sender vehicle drives close to the receiver vehicle, and passes the vehicle to the place where the link is barely connected between two vehicles in 30 seconds. Figure 35 illustrates the SNR of the receiver, the on-demand adaptive channel estimator, rate adaptation, and the goodput of DORA and ARF. The on-demand adaptive estimator tracks the SNR of the receiver quite well with the average

UDP overhead of 0.94 messages per second. Since the actual SNR of the receiver is around 30dB, the estimator takes it as 10dB, and the rate adaptation stays at 1 Mbps in this channel. In Figure 36, detailed behavior of the optimal MPDU selection in DORA is depicted. The optimal MPDU L_{opt} follows the shape of the estimation in selecting MPUDs between 300 bytes, 500 bytes, and 750 bytes in 1 Mbps. For the ARF, the connection is barely sustained with the goodput of 0.8 Kbps, while DORA outperforms ARF with 615 Kbps in this low SNR channel.

For the second scenario, the sender controls the distance to the receiver to maintain approximately 10dB more than the previous channel in the Interstate 85 North, Exit 96 to 99. Thus, the average receiving power of the signal is approximately eight times greater than the previous low SNR channel. The on-demand estimator subtracts 25 dB for the compensation of the AWGN model against the Vehicle-to-Vehicle environments such that actual 40dB SNR is regarded as 15 dB for choosing L_{opt} and R_{opt}. In Figure 37, the
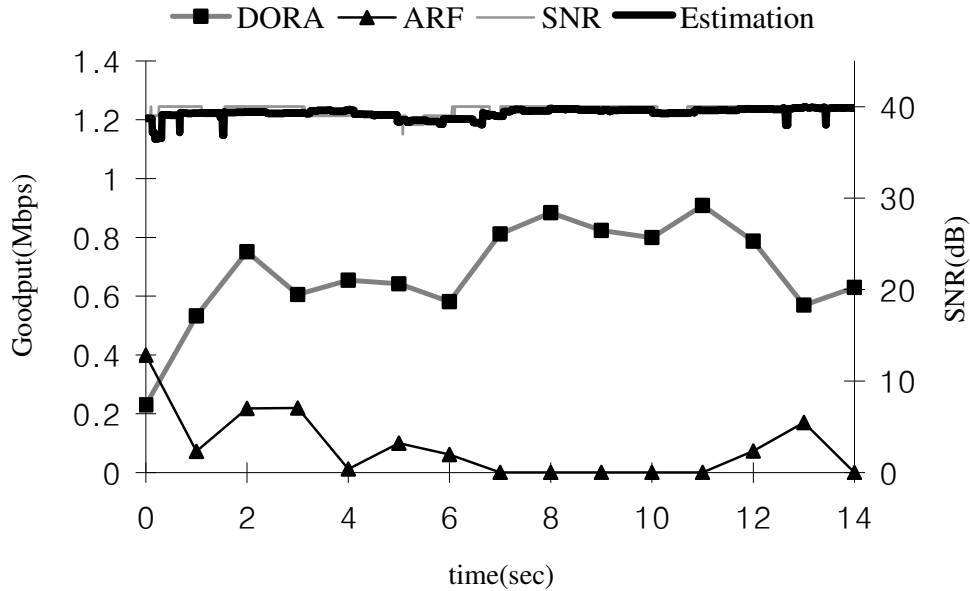

Figure 37. Illustration of high SNR channel performance in DORA and ARF.

estimator tracks the SNR with very little error. Based on this estimation, DORA selects L_{opt} and R_{opt} using Table 3. Since the initial SNR is 38 dB, the rate R_{opt} is maintained to 1 Mbps in Figure 38. When the SNR increases to 40dB at 15 seconds, the rate R_{opt} switches to 5.5 Mbps immediately. It fluctuates between 2 Mbps and 5.5 Mbps for roughly 10 seconds, and drops down to 2 Mbps at 25 second. Note that at 25 second, the SNR is 44dB while the estimation is 42.5 dB. This estimation error is the largest for the entire duration of the experiment while the average estimation error is just 0.15 dB with 1.0 UDP messages per second.

Fortunately, this estimation error does not affect the rate selection, since both 19 dB and 17.5 dB in the estimator for the SNR of 44 dB and 42.5 dB use the same transmission rate in Table 3. However this estimation error does change the optimal fragmentation from 1500 bytes to 300 bytes MPDU causing a little bit of the goodput
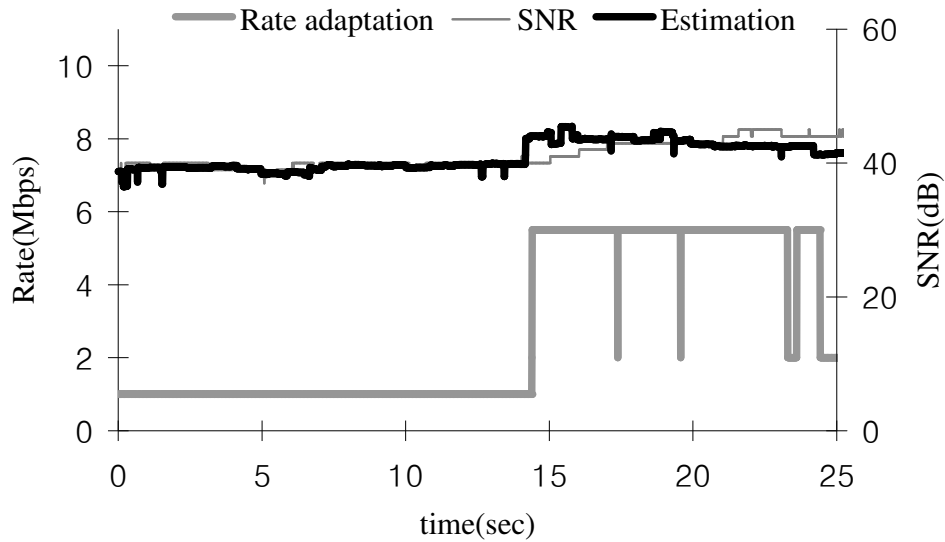

Figure 38. Adaptive channel adaptation and rate adaptation of DORA in a high SNR channel.

sacrifice. This overhead of the fragmentation is very minor, and the performance degradation is less than 1 % from the optimal value for a very short time duration, while

DORA still outperforms ARF with the average goodput enhancement of eight times for the entire duration of the experiment. The actual average goodput of DORA is 680 Kbps, and ARF is just 88 Kbps in this experiment. The selection of the optimal fragment L_{opt} is straight forward, and shown in Figure 39.

It is interesting to see that the SNR in this region is very strong even though the two vehicles maintain almost the same distance as the previous experiment. Additionally, the goodput in this experiment is just 10.5 % improved with 10dB SNR gain. Further analysis can be made through combining other wireless network parameters, such as mean excess delay and rms delay spread to define multipath components in this channel. Note that many vendors require a 65-ns rms delay spread to support full data rate in 802.11b. However detailed modeling of the wireless channel associated with multipath components is beyond the research scope of this study, and should be included for the future work.
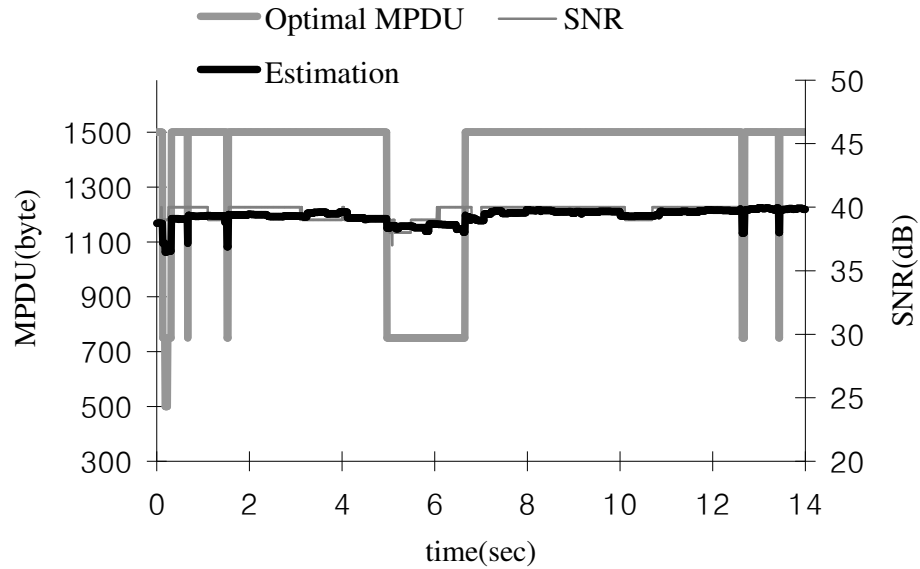

Figure 39. Adaptive channel adaptation and optimal MPDU selection of DORA in a high SNR channel.
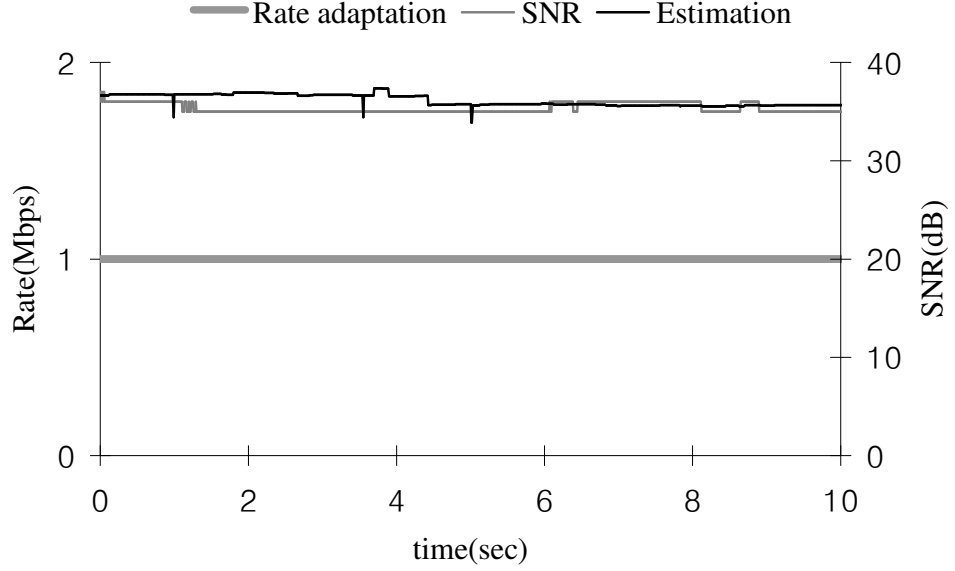
Figure 40. Adaptive channel adaptation and rate adaptation of DORA in a middle SNR channel.

For the last Vehicle-to-Vehicle scenario, the SNR is set to approximately 35dB in the Interstate 85 North, Exit 91 to 94. The on-demand estimator subtracts 25 dB as the second experiment. The SNR of the receiver, the adaptive channel estimation, and the rate adaptation of DORA is illustrated in Figure 40. Since the SNR of the receiver is around 35 dB, the estimator assumes it as 10 dB, and the rate is selected to 1 Mbps. The average estimation error of this channel is 0.6dB with the overhead of 0.95 messages per second.

The optimal MPDU selection is shown in Figure 41. The selection of L_{opt} is more sensitive than the rate R_{opt} in terms of the decision range of the SNR. The largest error for the entire duration of the experiment is 2.3 dB at four second. This estimation error switches L_{opt} from 750 bytes to 1500 bytes, resulting in 4 % goodput degradation from the optimal fragment. However, this only happens when the estimation error is large enough to cross the borderline between the rates and optimal fragments, and causes more
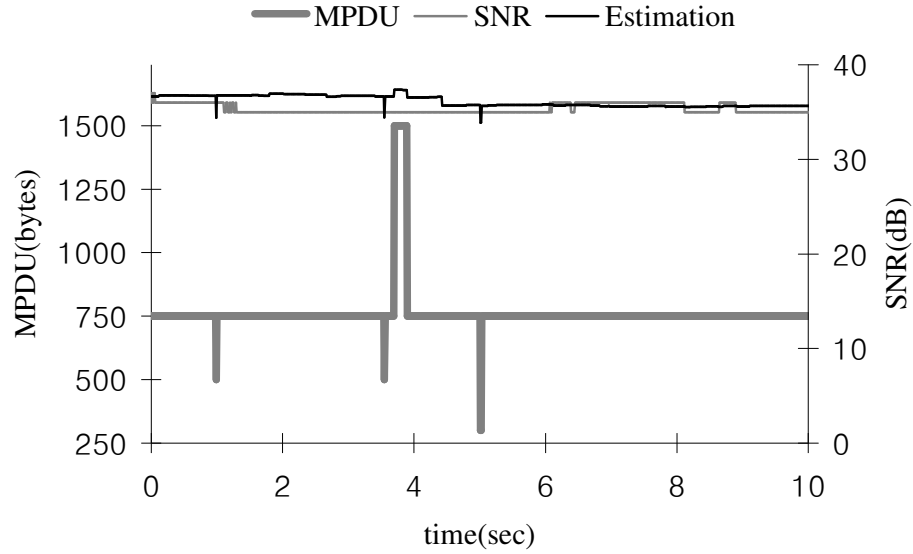
**Figure 41. Adaptive channel adaptation and optimal MPDU selection of DORA
in a middle SNR channel.**

serious goodput deterioration when the estimation values are greater than the actual SNR

of the receiver. Note that using one larger fragment degrades the performance more than

using one smaller fragment for the same SNR. Based on the observations and results

from the experiments, this estimation error rarely happens for a very short time. The

instantaneous goodput for this time duration, nevertheless, is still equal or greater than

ARF. In fact, the results show 74% improvement of the goodput in the period. Overall,

the average goodput of DORA is 627 Kbps while ARF is 325.6 Kbps as shown in Figure

42.

The performance of DORA and ARF vs. the SNR of the receiver in Vehicle-to-

Vehicle is illustrated in Figure 43. The goodput of DORA is proportional to the quality of

the SNR while ARF shows inconsistent relationship with it. It is very hard to explain this

inconsistent phenomenon of ARF only with the SNR and goodput relationship in MAC

and Physical layers. Mean excess delay and rms delay spread to define multipath
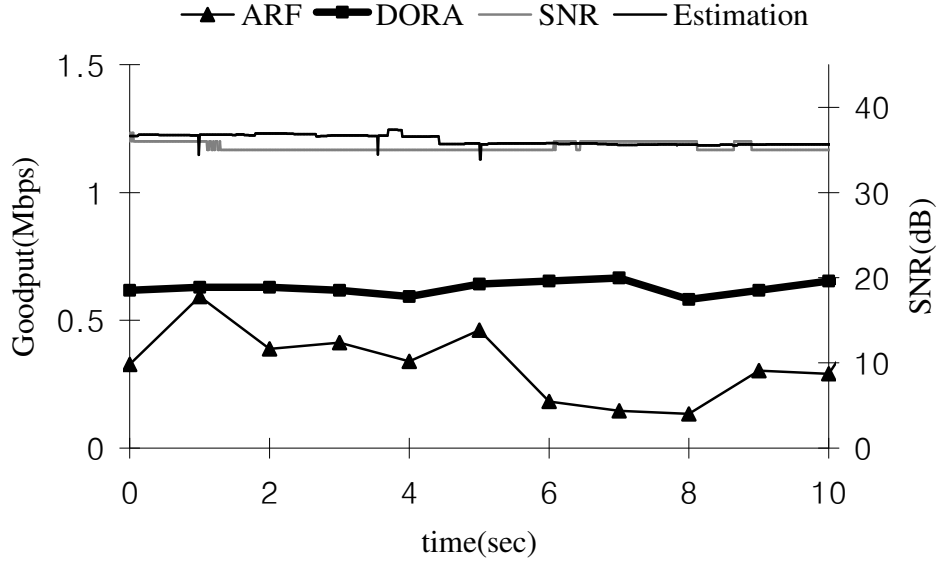
Figure 42. Illustration of middle SNR channel performance in DORA and ARF.
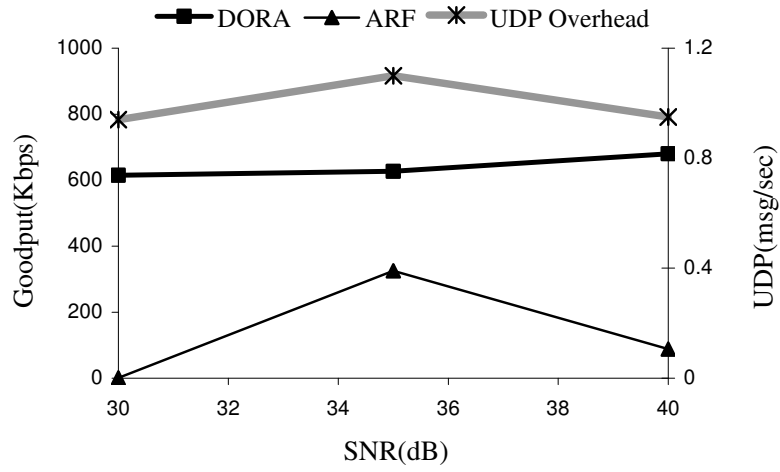
Figure 43. Performance of DORA and ARF with UDP overhead in Vehicle-to-Vehicle networks.

components can be incorporated in the proposed model (13) to anticipate more precise analysis for outdoor wireless mobile channels. In addition, the transport layer protocol in

this experiment is TCP, which assumes packet losses are an indication of network congestion. TCP is well known to have inability to hold efficiency in wireless networks, and performs poorly by reducing the congestion window when packet losses occur due to wireless link characteristics. Therefore, thorough analysis of TCP interaction with MAC and Physical layer characteristics in wireless channel is important and should be included in future research.

CHAPTER 7

CONCLUSIONS AND FUTURE RESEARCH

In this thesis, an effective way to increase the system goodput of CSMA/CA MAC in wireless mobile networks is presented. The proposed model reveals the impact of the number of contending stations, the packet collisions, the packet error probability, and the fragmentation overhead on the system goodput. Using an adaptive on-demand SNR estimator, dynamic optimal fragmentation with rate adaptation (DORA) dynamically selects the optimal rate and fragmentation in time varying channels with minimal overhead. Through rigorous analysis and extensive experiments, DORA enhances the goodput approximately 18% in a typical WLAN environment, 48% in ad hoc networks and 464% in Vehicle-to-Vehicle networks. The proposed protocol is an energy-efficient model applicable to any CSMA/CA MAC protocol for next generation wireless networks, and a realistic approach that can be deployed without modification of the standards.

7.1 Research Contributions

In the thesis, a generic CSMA/CA MAC operation with a comprehensive analytical model is proposed. This model includes the following features.

- Single and multi users with the analysis of contention and collision probabilities.

- Normal and fragmentation operation with the consideration of the overheads.

- Perfect and error prone channels with the analysis of packet error rates.

- Arbitrary packet lengths.

In addition to the proposed model, a novel on-demand adaptive estimator is developed and experimented to provide the SNR of the receiver in wireless mobile environments. The advantages of the estimator includes the following:

- Extremely low overheads: average of less than one 2 bytes UDP messages per second in highway driving experiments.

- Average estimation error is less than 0.6 dB per sample.

- Very simple to implement, and no protocol modification is required.

- Adjustable parameters for adapting to wireless environments.

To evaluate the performance of DORA, test-beds are developed and extensive experiments are executed in WLAN, ad hoc networks, and Vehicle-to-Vehicle networks.

In WLAN, packet losses are a major obstacle achieving higher goodput in a bad BER channel, and smaller fragments have more benefit than the drawback of the overhead in the channel.   By choosing these optimal values, the maximum goodput can be obtained by using DORA. The benefits of using DORA in WLAN are summarized as follows.

- For a moderate BER of 1×10^{-5}, 18.4% of goodput is improved.

- In error prone channel, BER of 1×10^{-4}, 73% of goodput is enhanced.

For the ad hoc networks, the experiments show that DORA with transmission power control can accomplish considerable performance improvement. Strong signals introduce severe interference to the adjacent links, and prohibit the other stations from routing the packets at the same time. Thus, by reducing the transmission power, the interference reduces significantly, and DORA performs better in this low SNR channel.

As a result, DORA provides a more energy efficient routing algorithm with less transmission power and accomplishes the following.

- For a moderate BER of 1×10^{-5}, 48.1% of goodput is increased.

In Vehicle-to-Vehicle Networks, the goodput of DORA is proportional to the quality of the SNR while ARF shows inconsistent relationship in a low SNR channel. The advantages of using DORA in these channels are more dramatic than the other environments in WLAN and ad hoc. This resulted from dynamically changing environments in highways with trucks, different curvature and elevation of the road. The experiment shows following.

- For the SNR of 30dB to 40dB, 464% of goodput enhancement is achieved.

7.2 Limitations and Future Research

There are a lot of assumptions and approximation of the proposed algorithm, which makes difficult to anticipate precise results between the model and the reality.

First of all, the proposed model (13) computes the optimal fragmentation and the transmission rate based on the assumptions that the unsuccessful transmission probability is constant at steady state in a generic slot. This is valid only if the backoff stage of the whole system is at steady state. Additionally, the probability of the packet loss in (6) is related to BER with its upper bound. This introduces differences between the probability and the actual dropped packets by random bit errors in the experiments.

In estimating the BER from the measured SNR in the experiments, equation (19) is used for an additive white Gaussian noise channel. Similarly, the approximated symbol error rate of DQPSK and CCK is also used over an AWGN channel to decide R_{opt} and L_{opt}. The AWGN channel model is not realistic in these environments. Nevertheless, the

model is used for reference purposes, since no exact channel models are known for the places where the experiments are executed. Note that it is straightforward to apply new models to relate the SNR and the BER or SER to determine R_{opt} and L_{opt}, if they are available in future.

For future research, the parameters of the estimator can be optimized such that the estimation error is further reduced in different environments. Based on these findings, the parameters can dynamically adapt to the channels to minimize the error in real time.

In ad hoc networks, research can be performed to find optimal routing path over wireless ad hoc networks to maximize goodput. Note that DORA is to optimize one-hop wireless link rather than end-to-end routing path, and it provides maximum achievable goodput of each link for the established routing path. However, this path may not be the best route in terms of maximum goodput. Therefore, finding the best routing path that incorporates individual optimized links to the last-hop is a challenging problem due to difficulty of exhaustive search for the possible routing paths among many nodes in dynamic mobile ad hoc networks. An analysis of end-to-end performance along the optimized links in ad hoc networks with TCP interaction can be considered for future research as well.

The goodput of DORA is proportional to the SNR while ARF shows inconsistency in Vehicle-to-Vehicle networks. Mean excess delay and rms delay spread to define multipath components might be useful to anticipate more precise analysis in (13) for outdoor wireless vehicular channels. In addition, thorough analysis of TCP interaction with the multipath components needs to be investigated when TCP reduces the congestion window due to the packet losses in wireless links. All these researches

will lead us to design robust TCP algorithms for wireless networks, and allow us to produce efficient routing, MAC, and Physical layer protocols for faster yet reliable data communication in future wireless mobile networks.

REFERENCES

[1] IEEE Std 802.11b-1999, Wireless LAN Medium Access Control (MAC) and Physical Layer (PHY) Specification: High-speed Physical Layer Extension in the 2.4GHz Band, P802.11, 1999.

[2] IEEE Std 802.11a-1999, Wireless LAN Medium Access Control (MAC) and Physical Layer (PHY) Specification: High-speed Physical Layer Extension in the 5GHz Band, P802.11, 1999.

[3] IEEE Std 802.11g-2003, Wireless LAN Medium Access Control (MAC) and Physical Layer (PHY) Specification: Further Higher Data Rate Extension in the 2.4GHz Band, Amendment to IEEE 802.11 Std, Jun. 2003.

[4] A. Kamerman and L. Monteban. "WaveLAN-II: A high-performance wireless LAN for the unlicensed band. Bell Labs Technical Journal, pages 118-133, summer 1997.

[5] G. Holland, N. Vaidya, and P. Bahl, "A rate-adaptive MAC protocol for wireless networks," in Proc. ACM MOBICOM'01, Jul. 2001, pp. 236-251.

[6] B. Sadeghi, V. Kanodia, A. Sabharwal, and E. Knightly, "Opportunistic media access for multirate ad hoc networks," in proc. ACM MOBICOM'02, Sep. 2002, pp.24-35.

[7] P. Lettieri and M. B. Srivastava, "Adaptive Frame Length Control for Improving Wireless Network Link Throughput, Range and Energy Efficiency," Proceedings of the IEEE INFOCOM 1998, March 1998.

[8] S. Ci and h. Sharif, "Adaptive approaches to enhance throughput of IEEE 802.11 wireless LAN with bursty channel," in Proc. IEEE LCN'00, Nov. 2000, pp. 44-45.

[9] J. Tourrihes, "Dwell adaptive fragmentation: How to cope with short dwells required by multimedia wireless LANs," in Proc. IEEE GLOBECOM'00, VOL. 1, 2000, PP. 57-61.

[10] J. Tourrihes, "Fragmentation adaptive reduction: Coping with various interferers in radio unlicensed bands," in Proc. IEEE ICC'01, VOL. 1, 2001, PP. 239-244.

[11] D. Qiao and S. Choi, "Goodput Enhancement of IEEE 802.11a Wireless LAN via Link Adaptation," Proc. IEEE International Conference on Communications, June 2001.

[12] D. Qiao and S. Choi, and K. G. Shin, "Goodput analysis and link adaptation for IEEE 802.11a wireless LANs," IEEE/ACM Transactions on Mobile Computing, vol. 1, pp. 278-291, Dec. 2002.

[13] J. Yin, X. Wang and D.P. Agrawal, "Optimal Packet Size in Error-prone Channel for IEEE 802.11 Distributed Coordination Function," in Proc. The 2004 IEEE Wireless Communications and Networking Conference (WCNC'04), Atlanta, 21-25 March 2004.

[14] B. Kim, Y. Fang, T. Wong, and Y. Kwon, "Throughput Enhancement Through Dynamic Fragmentation in Wireless LANs," IEEE Transactions on Vehicular Technology, Vol. 54, No. 4, July 2005.

[15] G. Bianchi, "Performance Analysis of the IEEE 802.11 Distributed Coordination Function," *IEEE Journal on Selected Areas on Communications,* Vol. 18, No. 3, March, 2000.

[16] J. Case, M. Fedor, M. Schoffstall, J. Davin, A Simple Network Management Protocol (SNMP). Request for Comments 1157, Internet Engineering Task Force, May 1990.

[17] F. Cali, M. Conti and E. Grergori, "Dynamic Tuning of the IEEE 802.11 Protocol to Achieve a Theoretical Throughput Limit," IEEE/ACM Transactions on Mobile Compting, Vol. 1, No. 1, Jan-Mar. 2002.

[18] J. L. Joshua, "Very Low Power Wireless Protocol Performance," M. S. thesis, Tufts University, May 2000.

[19] T.S. Rappaport, "Mobile radio propagation: Large-scale path loss," in Wireless Communications: Principles and Practices. Upper Saddle River, NJ: Prentice-Hall, 1996, pp. 69-185.

[20] J. G. Proakis and M. Salehi, "Differential phase modulation and demodulation," in *Comtemporary Communications Systems Using Matlab*. Piscataway, NJ: Brooks/Cole Thomson Learning, 2000, pp. 302-309.

[21] J. G. Proakis, "Performance of the optimum receiver for memoryless modulation," *Digital Communications*, 3rd ed., New York, NY: McGraw-Hill, 1995, PP 257-282.

[22] T.S. Rappaport, "Mobile radio propagation: Small Scale Fading and Multipath," in Wireless Communications. NJ: Prentice-Hall, 1996, pp. 139-192.

[23] Cisco Aironet 1231G-A-K9, http://www.cisco.com.

[24] X. Li, P. Kong and K. Chua, "Analysis of TCP in IEEE 802.11 Based Multi-hop Ad Hoc Networks," in *Proc. ICCCN'05*, Oct. 2005, pp. 297-302.

[25] IEEE P802.11p: Wireless Access in Vehicular Environment (WAVE), draft standard ed., IEEE Computer Society, 2006.

[26] http://www.haicom.com.tw/gps303E.shtml.

[27] http://www.gps2traveltime.com/GPS2PDA/gps2pda.html.

[28] http://www.jamartech.com/pctravel.html.

[29] http://www.ubuntu.com.

VITA

Yusun Chang

Yusun was born in a small town, Mongtan, a southern province of Korea in 1971. He attended Korea Aerospace University, and received a B.S. and M.S. in Avionics in 1993, and 1995 respectively. He served air force as an instructor for four years, and came to the U.S. to study in 2000. He received a M.S. in Electrical Engineering at Columbia University in New York, and worked at Bell Lab before coming to Georgia Tech for a doctorate in 2002. In 2007, he received his Ph. D. in Electrical and Computer Engineering from Georgia Institute of Technology. His research interest includes modeling and performance analysis of wireless mobile networks, and optimization and implementation of wireless communication system.

Mr. Yusun loves to read books, especially history, politics, and international relations articles. He has been playing classic guitar for 20 years, and likes to play golf and tennis when the sun shines.